Petroleum Science 20 (2023) 3766–3782

Contents lists available at ScienceDirect

Petroleum Science

journal homepage: www.keaipublishing.com/en/journals/petroleum-science

Original Paper

Prediction of pressure gradient and hold-up in horizontal liquid-liquid pipe flow

Syed Amjad Ahmed [a, b], Bibin John [a, *]

[a] School of Mechanical Engineering, Vellore Institute of Technology, India
[b] Department of Mechanical Engineering, C Abdul Hakeem College of Engineering & Technology, India

ARTICLE INFO

Article history:
Received 20 December 2022
Received in revised form
21 March 2023
Accepted 1 July 2023
Available online 8 July 2023

Edited by Jia-Jia Fei

Keywords:
oil-water flow
two-fluid model
pressure gradient
stratified flow
dispersed flow

ABSTRACT

This paper aims to propose correlations to predict pressure gradient, friction factor and fluid phase hold-up in liquid-liquid horizontal pipe flow. To develop the correlations, experiments are conducted using high viscous oils (202 and 630 mPa·s) in a steel pipe of length 11.25 m and length-to-diameter ratio of 708. In addition, the experimental data from the literature comprising wide range of flow and fluid properties is analyzed. For the analysis, the liquid-liquid pipe flow data is categorized into two as: stratified and dispersed. The existing friction factor correlations are modified to incorporate the effects of viscosity of the oil phase, interfacial curvature (contact/wetting angle-in lieu of material of the pipe) and fluid phase fraction. In the two-fluid model of stratified flow, the wall stress and interfacial stress correlations are substituted with superficial velocities of fluids and superficial Reynolds numbers of fluid phases replacing fluid phase velocities and fluid Reynolds numbers. Similarly, for dispersed flow, an effective Reynolds number is described as the sum of superficial Reynolds number of oil and water phases. Substituting the generally employed mean or mixture Reynolds number with the effective Reynolds number into the existing single-phase turbulent flow friction factor correlation, an effective friction factor for oil-water flow is proposed. Employing the proposed correlations, the pressure gradient across the oil-water flow and hold-up volume fraction are predicted with significant reduction in error compared with that of conventionally employed correlations. The average error and standard deviation values of −7.06%, 20.72% and 0.31%, 18.79% are found for stratified flow and dispersed flow respectively.

1. Introduction

The comprehension and the accurate prediction of the pressure gradient across liquid-liquid pipe flow is crucial for the efficient design and operation of many industrial processes like transportation of oil, separators and heat exchangers etc. In such applications, the determination of flow pattern, hold-up, pressure gradient and other parameters are critical for the design and flow assurance issues. Among the influencing parameters, the pressure gradient across the oil-water flow is the most significant for process intensification (Hapanowicz, 2021). Consequently, the pressure gradient characteristics across the flow have been under investigations for more than five decades (Wright, 1957; Charles et al., 1961; Ward, 1964; Dukler et al., 1964; Guzhov et al., 1973; Martinez et al., 1988; Trallero et al., 1997; Angeli and Hewitt, 1998; Elseth, 2001; Chakrabarti et al., 2005; Sotgia et al., 2008; Grassi et al., 2008; Strazza et al., 2011; Al-Wahaibi et al., 2007a, b; Yusuf et al., 2012; Rodriguez and Baldani, 2012; Dasari et al., 2014; Yang, 2014; Edomwonyi-Otu and Angeli, 2014; Shi and Yeung, 2016; Yang et al., 2021).

The pressure gradient characteristics of liquid-liquid pipe flow, in general, depends on the flow patterns (stratified, semi-dispersed, dual-continuous and dispersed). Here, the stratified flow refers to the flow of less dense fluid (generally oil) atop of the high dense fluid. With the interface become unstable at higher flow rates and droplets emerging at the interface, the flow pattern is referred as stratified flow with mixing interface (STMI) (Trallero et al., 1997). When the droplets of one fluid are found into the other phase, the flow patterns are referred as semi-dispersed (dual-continuous). The fully dispersed is referred as the flow when fine dispersion of one fluid into the other is observed (Brauner, 2001). A detailed description on the classification of flow patterns is presented by

* Corresponding author.
E-mail address: bibin.john@vit.ac.in (B. John).

https://doi.org/10.1016/j.petsci.2023.07.001

Ibarra et al. (2014). Consequently, the two-fluid model and homogenous model are respectively employed for stratified and dispersed flows. However, it is found to be rather equivocal on the appropriate model to be employed for the semi-dispersed and dual-continuous liquid-liquid pipe flow (Oliemans, 2011), since these flow patterns exhibit both stratified and dispersed features.

The review of the liquid-liquid pipe flow indicates that the pressure gradient is dependent on flow rates, fluid phase properties and characteristics of pipes. In addition to the flow and fluid parameters, wettability characteristics of the pipe wall by the fluid phases affects the pressure drop substantially (Angeli and Hewitt, 1998). For example, Angeli and Hewitt (1998), for similar pipe diameter, flow and fluid parameters, higher pressure gradient is observed for steel pipe than with the acrylic pipe. Similarly, Yusuf et al. (2012) noted that the fluid fraction and fluid velocities play an important role on the pressure drop characteristics. Also, the phase inversion phenomenon and the effective viscosity affects the pressure gradient across the liquid-liquid flow (Mukhaimer et al., 2015).

1.1. Pressure gradient in liquid-liquid pipe flow

The effect of pipe material is evident from the experimental data of oil-water flow in acrylic and steel pipes by Angeli and Hewitt (1998). In addition, the data of Liu et al. (2008) may be compared with that of Chakrabarti et al. (2005). Though the experimental data of Liu et al. (2008) and Chakrabarti et al. (2005) at exactly the same flow conditions is not available, the data is compared for very similar conditions. For example, for data of Chakrabarti et al. (2005), when the flow conditions are $U_{so} = 0.06$ m/s and $U_{sw} = 0.15$ m/s, the pressure gradient is 31.44 Pa/m. For a similar flow condition of $U_{so} = 0.05$ m/s and $U_{sw} = 0.14$ m/s, the pressure gradient observed by Liu et al. (2008) is 55 Pa/m. That is, higher pressure gradients are observed in steel pipe compared to that of acrylic pipe. Therefore, it may be inferred that the hydrophilic/oleophobic pipes (steel) give higher pressure gradient than that of hydrophobic/oleophilic (acrylic/plastic) pipes (also refer dos Santos et al., 2006).

Similarly, with viscosity of oil phase, the pressure gradient across the liquid-liquid pipe flow tend to increase. The work of Vielma et al. (2008), Yusuf et al. (2012), Dasari et al. (2014), Rodriguez et al. (2012) and Rodriguez and Baldani (2012) have not only shown higher pressure gradients compared with low viscosity oil-water flows, but entirely different characteristics. The increase of water phase volume fraction increases the pressure gradient in low viscous oil ($\approx$2 mPa•s). However, in contrast, the pressure gradient decrease with water volume fraction for high viscous oil-water flows. Note that both the viscosity of the oil phase and the material of the pipe affect the wetting property and hence affect the interfacial curvature and the area occupied by each fluid phase.

There are many analytical and empirical models available in the literature of two phase pipe flow to describe the pressure gradient across the flow. These models are basically developed for gas-liquid pipe flow and subsequently adapted for liquid-liquid pipe flow. For example: i) homogeneous no-slip flow model by Wallis (1969), ii) drift-flux model (Zuber and Findlay, 1965), iii) the two-plate model with flat interface (Ullmann et al., 2004; Brauner, 2001), iv) the two-fluid model (Brauner et al., 1998) and v) empirical models (Charles and Lilleleht, 1966). These correlations are extended to oil-water flows and thus, the frictional pressure gradient (Rodriguez et al., 2012) and the affecting parameters are characterized. Further, empirical correlations and correlation using dimensional analysis (Dasari et al., 2014) were proposed for oil-water flow. However, many of such correlations are found to be erroneous when employed for the experimental data beyond the range of the data from which they are constructed.

The analytical investigation of stratified flows is generally carried out using the two-fluid model. The model is a one-dimensional steady-state momentum equation of the two fluid phases. In other words, the two-phase pressure drop is presented by using single-phase pressure drop of the individual liquid phases. The momentum balance for oil phase and water phase flowing in the pipe may be given as (refer Fig. 1 below):

$$A_o\left(-\frac{\partial P}{\partial z}\right) - \tau_o S_o \pm \tau_i S_i - A_o \rho_o g \sin\beta = 0 \tag{1}$$

$$A_w\left(-\frac{\partial P}{\partial z}\right) - \tau_w S_w \pm \tau_i S_i - A_w \rho_w g \sin\beta = 0 \tag{2}$$

where P is pressure, z is the axial coordinate, β is the angle made with horizontal, g is the acceleration due to gravity, A_o and A_w are the cross-sectional areas occupied by oil and water, S_o and S_w are the arc lengths of the pipe wall covered by oil and water, τ_o and τ_w are the shear stresses exerted at the pipe wall by the oil and water, S_i and τ_i are the interfacial arc length and interfacial shear stress, respectively.

The two-fluid model, Eq. (1) and Eq. (2), is supported by appropriate closure equations at the wall and the interface. The closure relations required for the wall and interfacial shear stress are generally in terms of friction factor (Brauner et al., 1998; Brauner, 2001). Employing these parameters for horizontal flow ($\beta = 0$) and considering $U_o \approx U_w$, the pressure gradient across the liquid-liquid pipe flow and the hold-up volume fraction may be determined using,

$$\left(\frac{\partial P}{\partial z}\right) = \left(\frac{-\tau_o S_o - \tau_w S_w}{A_o + A_w}\right) \tag{3a}$$

$$\frac{\tau_o S_o}{A_o} - \frac{\tau_w S_w}{A_w} + \tau_i S_i\left(\frac{1}{A_w} + \frac{1}{A_o}\right) = 0 \tag{3b}$$

Here, the shear stresses at the wall (τ_w and τ_o) and interfacial stress (τ_i) are calculated (Edomwonyi-Otu and Angeli, 2014; Al-Wahaibi, 2012) using

$$\tau_w = \frac{f_w \rho_w U_w^2}{2};\ f_w = m\, Re_w^{-n} \tag{4a}$$

$$\tau_o = \frac{f_o \rho_o U_o^2}{2};\ f_o = m\, Re_o^{-n} \tag{4b}$$

$$\tau_i = \frac{f_i \rho_f (U_w - U_o)^2}{2}; \tag{4c}$$

$$\begin{cases} f_i = f_w \text{ and } \rho_f = \rho_w \text{ for } U_w > U_o \\ f_i = f_o \text{ and } \rho_f = \rho_o \text{ for } U_w < U_o \end{cases}$$

$$Re_w = \frac{\rho_w U_w D_{hw}}{\mu_w} \tag{4d}$$

$$Re_o = \frac{\rho_o U_o D_{ho}}{\mu_o} \tag{4e}$$

where U_w and U_o are water and oil phase velocities and D_h is hydraulic diameter of pipe defined for oil and water phase as:

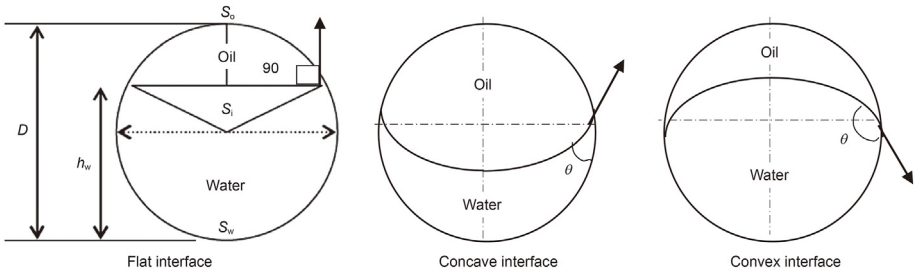

Fig. 1. Representation of geometric parameters and interfacial shapes.

$$D_{hw} = 4A_w/(S_w + S_i)$$

$$D_{ho} = 4A_o/(S_o + S_i)$$

The constants m and n are: either 0.046 and 0.2 (Knudsen and Katz, 1954; Brauner, 2001) or 0.0792 and 0.25 for turbulent regime and 16 and 1 laminar regime (Edomwonyi-Otu and Angeli, 2014). Using Fig. 1, the geometric parameters are described as (Edomwonyi-Otu and Angeli, 2014):

- Wall perimeter occupied by oil phase, $S_o = D\cos^{-1}\left(\frac{2h_w}{D} - 1\right)$
- Wall perimeter occupied by water phase, $S_w = \pi D - S_o$
- Interfacial length, $S_i = D\,[1-(2h_w/D-1)^2]^{0.5}$
- Cross section area of pipe filled by oil phase, $A_o = 0.25\,D\,[(S_o - S_i)(2h_w/D - 1)]$
- Cross section area of pipe, $A = (\pi/4)\,D^2$
- Cross section area of pipe filled by water phase, $A_w = A - A_o$
- Oil hold-up, A_o/A
- Water hold-up, A_w/A
- In-situ oil velocity, U_{so}/H_o
- In-situ water velocity, U_{sw}/H_w

and the corresponding friction factors (f_w and f_o). Re_w and Re_o are respective fluid Reynolds number. D_{hw} and D_{ho} are hydraulic diameter of water phase and oil phase.

While deriving the exact solutions for stratified oil-water pipe flows, assuming flat interface, for a given hold-up fluid fraction, Biberg and Halvorsen (2000) indicated that the interface curvature of horizontal flows are dependent on the viscosity ratio of the fluid phases. In this context, it may be noted that Ng et al. (2004) observed that due to the interactions of the oil and water at the interface and at the wall, the respective equivalent friction factors are quite inconsistent and indicated that the equivalent friction factors are difficult to formulate. Extending the two-fluid model, Chakrabarti et al. (2005) developed model by considering the minimization of the total two-phase system energy (phases have the same pressure drop). Further, by adapting the closure relations of Brauner et al. (1998), Chakrabarti et al. (2005) found the variations in pressure gradient predictions by 40%–200%. Similarly, Ullmann and Brauner (2006) proposed the empirical relations for the wavy-stratified flow pattern taking into consideration the effect of waves on the interface shear and found the pressure gradient within ±20% variation. Rodriguez and Oliemans (2006), incorporating the wave roughness into the two-fluid model, predicted the pressure gradients with an accuracy of 35%. On this, Oliemans (2011)noted that the average errors for the two-fluid model for stratified flow are in the 20%–40% range with errors exceeding 100%. Later, Rodriguez and Baldani (2012) established a new closure relation incorporating the constant-curvature arc as interface with high viscous oil-water flow in a glass pipe. A comprehensive analysis of two-fluid model was conducted by Edomwonyi-Otu and Angeli (2014) with stratified and stratified wavy flow patterns. Recently, Bochio et al. (2021) carried out investigation of high viscous oil-water flow using large eddy simulation (LES) and wire-mesh sensor to capture the interface to enhance the prediction of two-fluid model.

Note that, in the presently employed friction factor correlations in the literature for oil-water flow, the interfacial curvature (effect of pipe material) and the interfacial curvature are not incorporated. That is, in the literature of liquid-liquid flow, as mentioned above in section 1.1, the friction factor (f) employed is that of defined for single-phase flow. That is, $f = C/Re^n$ ($C = 16$ and $n = 1$ for laminar and $C = 0.0792$ and $n = -0.25$ for turbulent). Also, $C = 0.046$ and $n = -0.2$ for turbulent is recommended (Knudsen and Katz, 1954; Brauner et al., 1998). The values of constants and exponents (C and n) are derived from experimental data of either single phase flows or low viscous oil-water flow. While the Reynolds number of each phase is calculated using Re_w or Re_o (Eq. (4d) and Eq. (4e)), the interface is assumed flat. In reality the interface is rarely flat due to the material (contact angle or wetting angle) of the pipe and/or the viscosity of the oil phase. Consequently, the assumption of the flat interface is erroneous and possibly an error of ±15% in the Reynolds number due to the hydraulic diameter formulation (Ahmed and John, 2021a).

Further, for dispersed liquid-liquid pipe flow, in general, the homogeneous flow model is applied. The homogeneous model allows the two fluid phases to be considered as an equivalent single phase with averaged properties. As a result, the shear stresses are predicted using single phase friction factor equation, which are calculated by volume averaging the physical properties (viscosity and density) of fluid phases. That is:

$$\frac{dp}{dz} = -\frac{f_m \rho_m U_m^2}{2D} - \rho_m g \sin\beta \tag{5a}$$

where

$$\rho_m = \rho_w \varepsilon_w + (1 - \varepsilon_w)\,\rho_o \tag{5b}$$

$$\mu_m = \mu_w \varepsilon_w + (1 - \varepsilon_w)\,\mu_o \tag{5c}$$

$$\varepsilon_w = \frac{U_{ws}}{U_{ws} + U_{os}} \tag{5d}$$

$$Re_m = \frac{\rho_m U_m D}{\mu_m} \tag{5e}$$

$$\frac{1}{\sqrt{f_m}} = -2\log\left(\frac{\frac{k}{D}}{3.7} - \frac{4.518}{Re_m}log\left(\frac{6.9}{Re_m} + \left(\frac{\frac{k}{D}}{3.7}\right)^{1.11}\right)\right) \quad (5f)$$

Here, U_m is the mixture velocity, D as the diameter of pipe, k is the roughness of pipe, f_m is the mixture Fanning friction factor which is function of μ_m (mixture viscosity) and ρ_m is the mixture density (Martinez et al., 1988; Elseth, 2001). Yusuf et al. (2012) investigated the homogenous model and found that the model is appropriate for low oil viscosities. However, discrepancies are found when oil was continuous phase. By analyzing the pressure gradient data available in the literature, consisting of various flow patterns (stratified with interfacial droplets and dual continuous) and for a range of fluid properties (0.0016–0.028 N/m^2 and 790–875 kg/m^3), Al-Wahaibi (2012) proposed the modified friction factor of Zigrang and Sylvester (1985) for oil-water flow and referred as corrected friction factor (f_{cor}),

$$\frac{1}{\sqrt{f_{cor}}} = -2\log\left(\frac{\frac{k}{D}}{0.25} - \frac{4.518}{Re_m}\log\left(\frac{6.9}{Re_m} + \left(\frac{\frac{k}{D}}{0.25}\right)^{1.11}\right)\right) \quad (6a)$$

and

$$\frac{dp}{dz} = 2.4\left(\frac{f_{cor}\rho_m U_m^2}{2D}\right)^{0.8} \quad (6b)$$

Accordingly, the satisfactory prediction of the pressure gradient using equation (Eq. (6b)) is demonstrated.

Later, Dasari et al. (2014) developed correlations for the pressure gradient in oil-water flow i) by modifying the Lockhart–Martinelli and two-phase multiplier parameter and ii) using dimensionless analysis (Buckingham's Pi-theorem) (refer Eq. (7)).

$$\frac{\Delta P}{L} = 3.25 Re_{so}^{-1.15} Re_{sw}^{0.19}\left(\frac{\sigma}{U_{sw}\mu_w}\right)^{0.001}\left(\frac{U_{so}^2\rho_o}{D}\right) \quad (7)$$

where $\frac{\Delta P}{L}$, Re_{so}, Re_{sw}, U_{so}, U_{sw}, D, ρ, μ, σ are pressure gradient across the flow, superficial Reynolds number of oil, superficial Reynolds number of water, superficial velocity of oil phase and water phase, diameter of pipe, density and viscosity of oil and water and surface tension between the oil and water respectively. Further, note that the pressure gradient correlation proposed by Dasari et al. (2014) (Eq. (7)) effectively may be simplified as,

$$\frac{\Delta P}{L} = f_{o-w}*\left(\frac{U_{so}^2\rho_o}{D}\right) \quad (8a)$$

where $f_{o\text{-}w}$ is friction factor of oil-water flow and given as:

$$f_{o-w} = 3.25 Re_{so}^{-1.15} Re_{sw}^{0.19}\left(\frac{\sigma}{U_{sw}\mu_w}\right)^{0.001} \quad (8b)$$

The above equation is similar to that of existing general pressure gradient formulation,

$$\frac{\Delta P}{L} = f*\left(\frac{U^2\rho}{D}\right) \quad (8c)$$

Therefore, the pressure gradient correlation of Dasari et al. (2014) is indeed the general form of pressure gradient equation (refer Eq. (8a)) with a friction factor ($f_{o\text{-}w}$) for oil-water flow. The two-phase friction factor, $f_{o\text{-}w}$, is represented as function of superficial Reynolds number of oil and water phase and other dimensionless number consisting of viscosity of water and interfacial tension, Eq. (8b). Though, Dasari et al. (2014) takes parameters like interfacial tension into consideration, the contact or wetting angle was not considered. Here, note that the contact/wetting angle characterizes the interfacial curvature (in lieu of material of pipe) considering that Angeli and Hewitt (1998) found significant influence of pipe material on the pressure gradient of oil-water pipe flows.

Recently, Hapanowicz (2021) proposed an empirical relation on the pressure gradient with reference to single phase fluid flow, Eq. (9). The constant C and exponents ($n1$–$n5$) values are defined based on the flow pattern (dispersed w/o, dispersed o/w and stratified with mixing at the interface).

$$\frac{\Delta P_{2f}}{\Delta P_w} = C\cdot R_{dp}^{n_1}\cdot R_{cp}^{n_2}\left(\frac{\varphi_o}{\varphi_w}\right)^{n_3}\cdot\left(\frac{\Delta P_o}{\Delta P_w}\right)^{n_4}\left(\frac{\eta_o}{\eta_w}\right)^{n_5} \quad (9)$$

Though the above equation (Eq. (9)) do not provide the pressure gradient explicitly, it gives oil-water pressure gradient ratio with reference to the pressure gradient using solely the water phase. In summary, the analysis of experimental data available in the literature, reveals that the complexity of the liquid-liquid pipe flow is mainly considered due to: the wetting property of the fluids due to pipe material (Angeli and Hewitt, 1998), viscosity of oil phase (Liu et al., 2008; Dasari et al., 2014; Rodriguez and Baldani, 2012), flow patterns, fluid fraction and dynamics at the interface (Ng et al., 2004; Hapanowicz, 2021).

Accordingly, the objectives of the present work are as follows. To evaluate the two-fluid model replacing the fluid phase velocities (U_o and U_w) in the wall and interfacial stress equations with the superficial velocities (U_{so} and U_{sw}) of fluid phases for stratified oil-water flow. To perform dimensional analysis and incorporate the parameters like contact/wetting angle, viscosity of oil phase, and fluid volume fraction into the empirical friction factor correlations employed in the two-fluid model. Besides, to investigate dispersed flow using the effective oil-water Reynolds number defined as sum of superficial Reynolds number of water and oil phase.

In the present work, the flow patterns of oil-water flow are classified into two groups as: i) stratified (constitutes stratified, stratified wavy and referred as S) and ii) dispersed (consisting of dual-continuous and fully dispersed and referred as D). In the literature, the flow patterns like the dual-continuous (with stratification with dispersion of droplets in each fluid phase) flow pattern is considered ambiguous since it exhibits a semblance of both stratified and dispersed (Rodriguez et al., 2012). The experimental data (19 data sets-Table 1) available in the literature are employed for the present investigation. In addition, data obtained from the experiments conducted using high viscous oils (202 and 630 mPa•s) are analyzed.

2. Methods

2.1. Friction factor correlations - stratified flow

Incorporating the parameters that affect the oil-water flow mentioned above, the respective fluid phase Fanning friction factors may be described as a function,

$$f_w = f(U_{sw}, D, \rho_w, \mu_w, \theta, U_m, \mu_o) \quad (10a)$$

$$f_o = f(U_{ow}, D, \rho_o, \mu_o, \theta, U_m, \mu_w) \quad (10b)$$

Table 1
Experimental data (present experiments and data from literature).

Author	Diameter of pipe, mm	Material of pipe	Viscosity ratio, μ_o/μ_w	Density ratio, ρ_o/ρ_w	Flow pattern	Eötvös number, $\Delta\rho g D^2/8\sigma$	No. of data sets
Valle and Kvandal (1995)	37.50	Glass	2.3	0.794	D	–	10
Nadler and Mewes (1997)	59.00	Perspex	27	0.841	S, D	40.02	8, 16
Trallero et al. (1997)	50.13	Acrylic	29	0.850	S, D	12.66	11, 20
Angeli and Hewitt (1998)	24.00	Acrylic	1.6	0.801	S, D	8.47	9, 43
Angeli and Hewitt (1998)	24.30	Steel	1.6	0.801	S, D	8.47	3, 62
Elseth (2001)	56.30	Acrylic	1.64	0.790	S, D	18.78	8, 43
Lovick and Angeli (2004)	38.00	Steel	6.0	0.828	D	7.60	45
Chakrabarti et al. (2005)	25.00	Acrylic	1.2	0.787	S, D	3.63	45, 19
Rodriguez and Oliemans (2006)	82.80	Steel	9.38	0.783	D	94.67	20
Al-Wahaibi et al. (2007b)	14.00	Acrylic	5.5	0.828	S, D	1.04	18, 18
Vielma et al. (2008)	50.03	Acrylic	13.5	0.858	S, D	28.13	6, 46
Liu et al. (2008)	26.60	Steel	3.5	0.828	S, D	4.77	13, 25
Al-Yaari et al. (2009)	25.40	Acrylic	1.57	0.780	S, D	9.92	5, 17
Rodriguez et al. (2012)	26.00	Glass	100	0.860	D	–	33
Rodriguez and Baldani (2012)	26.00	Glass	280	0.828	S	4.27	6
Yusuf et al. (2012)	25.40	Acrylic	12	0.875	S, D	4.84	5, 47
Edomwonyi-Otu and Angeli (2014)	14.00	Acrylic	5.5	0.828	S	1.04	38
Dasari et al. (2014)	25.00	Acrylic, PMMA	107	0.889	S, D	3.48	14, 61
Bochio et al. (2021)	26.00	Glass	204	0.886	S	4.27	9
Present - R	15.90	Steel	202	0.901	S, D	1.20	12, 14
Present - Y	15.90	Steel	630	0.919	S, D	1.06	13, 15

The parameters in the above equations Eq. (10a) and Eq. (10b), are similar to that employed by Dasari et al. (2014) except the contact/wetting angle ratio (θ) and mean flow velocity (U_m). The dimensionless term for contact angle is defined as, $\theta_c = \frac{\theta}{90}$. Here, the denominator value of 90° is angle of flat interface which is taken as reference to non-dimensionalize the contact angle (Fig. 1). Note that, in the present analysis, the interfacial tension (σ) is not included considering that Wahid et al. (2021) demonstrated the insignificance of interfacial tension. Accordingly, the dimensional analysis signifies that the fluid phase friction factor (f_w and f_o) correlations as a function of wetting angle, fluid volume fraction, superficial Reynolds numbers of oil and superficial Reynolds number of water and given as:

$$f_w = A\,(Re_{sw})^a\,(\theta_c)^b\,(\varepsilon_w)^c\left(\frac{\mu_o}{\mu_w}\right)^d \tag{11a}$$

$$f_o = A\,(Re_{so})^a\,(\theta_c)^b\,(\varepsilon_w)^c\left(\frac{\mu_o}{\mu_w}\right)^d \tag{11b}$$

Here, the constant A and the exponent's a, b, c and d may be determined employing the data of the present experiments and the data from the literature. Due to the consideration of superficial fluid velocities (U_{sw} and U_{so}) as parameters, note that the dimensional analysis results in the superficial Reynolds number (Re_{sw} and Re_{so}) and not fluid phase Reynolds number (Re_o and Re_w).

2.1.1. Wall and interfacial stresses defined

In the literature, for two-fluid model, the usage of fluid phase Reynolds numbers (Re_o and Re_w) (Eq. (4d) and Eq. (4e)) in friction factor correlations and phase fluid velocities (U_w and U_o) in the wall stress and interfacial stress correlations is the practice. However, in the present work, the mean velocity (U_m) to describe the wall stresses (τ_w and τ_o) and the superficial velocities of fluid phases to describe the relative momentum between the fluid phases at the interface are chosen. The primary rationale for this consideration is as follows. The fluid phase velocities (U_w and U_o) are unknown and are generally calculated using the fluid volume fraction ($U_o = U_{so}/H_o$ and $U_w = U_{sw}/H_w$). Here, U_{sw} and U_{so} are superficial velocities of water phase and oil phase respectively. H_o and H_w are hold-up fraction of respective oil phase and water phase. In particular, at low fluid volume fraction, the fluid velocities (U_o and U_w) obtained using the in-situ fluid velocity equations (given in section 1.1 above) are implausible. For example, for the data of Trallero et al. (1997), at superficial velocities $U_{sw} = 0.02$ m/s and $U_{so} = 0.25$ m/s, the fluid phase velocity U_w and U_o are found to be 0.61 and 0.26 m/s respectively. The water phase attaining $U_w = 0.61$ m/s is unlikely given that the mean velocity of flow is around $U_m = 0.27$ m/s. Further, with the volume fraction of water phase just less than 10% and flowing at the bottom of the pipe near wall (no-slip), the velocity of water phase as $U_w = 0.61$ m/s certainly improbable.

To further corroborate this aspect, the instantaneous velocity profiles obtained by Elseth (2001) and Ibarra et al. (2018) may be examined. From these instantaneous oil-water flow velocity profiles, for low water volume fraction, though the oil phase velocity (U_o) is 1.5 times of mean flow velocity ($\approx 1.5U_m$) at the center of pipe, the water phase velocity (U_w) may only approximate to the mean flow velocity ($\approx U_m$). Therefore, the water phase velocity at low water volume fraction exceeding the mean flow velocity many times is not only unlikely but erroneous. In actual, the fluid phase velocities do not linearly change with the geometric cross section occupied by the fluid phase. Rather, the fluid phases tend to retain the mean velocity of flow with no-slip at the wall. That is, $U_o \approx U_w \approx U_m$ (Hapanowicz and Polaczek, 2013). Therefore, it may be inferred that the fluid phase velocity, at low fluid volume fraction, calculated using respective fluid volume fraction is rather a *"geometrical construct"* and such fluid phase velocities are not found in practice. Thus possibly resulting in very high errors of ranging 100%–200% (Oliemans, 2011) in the prediction of pressure gradient. Incidentally, the high errors are found only at low fluid volume fractions.

In addition, the analytical rationale for this modification may be inferred from the following. Clausse and de Bertodano (2021) indicated that the mixture (mean) velocity of flow and relative velocity between the fluid phases satisfies the natural motion modes (yields non-elliptical equations) towards solving the ill-posedness of the two-fluid model. Consequently, in the wall stress correlation given above, the average velocities of respective fluid phase are replaced by the mean velocity of flow (U_m) defined as the sum of superficial velocity of water and oil ($U_m = U_{so} + U_{sw}$).

Further, as suggested by Clausse and de Bertodano (2021), that the relative motion between fluid phases should be represented by a parameter that satisfactorily characterizes respective transport phenomenon rather than an "auxiliary variable" that is determined from mixture variables and the fluid volume fractions. Accordingly, the interfacial stress correlation proposed in the present work (Eq. (12c)) is also incorporated with superficial velocities of oil and water phase replacing the fluid phase velocities. It may be noted that Eq. (12c) indicates the kinetic energy/momentum exchange at the interface. For further details on the mathematical analysis may be referred from Clausse and de Bertodano (2021).

Employing the proposed friction factors correlations, Eq. (11a) and Eq. (11b), the respective wall stresses (τ_w and τ_o) and interfacial stress (τ_i) may be determined as,

$$\tau_w = \frac{f_w \rho_w U_m^2}{2} \tag{12a}$$

$$\tau_o = \frac{f_o \rho_o U_m^2}{2} \tag{12b}$$

$$\tau_i = \frac{\varepsilon_f \left(f_o \rho_o U_{so}^2 - f_w \rho_w U_{sw}^2 \right)}{2} \tag{12c}$$

where $\varepsilon_f = \begin{cases} \varepsilon_w, \varepsilon_w \geq 0.5 \\ \varepsilon_o, \varepsilon_w < 0.5 \end{cases}$, and therefore, the pressure gradient of stratified oil-water flow using the two-fluid model may be determined using Eq. (3). Also, the recent work of Dorao et al. (2018), Ahmed and John (2021b) on the oil-water flow heat transfer characteristics noted that the effective Reynolds number (based on the superficial Reynolds numbers) of two-phase flow systems better describes the oil-water flow and results in the enhanced prediction of the heat transfer characteristics.

2.2. Effective friction factor – dispersed flow

The flow patterns constituting dual-continuous, semi-dispersed and fully dispersed are categorized as dispersed and hence homogeneous model is applied. In the literature, the homogenous model is applied to the flow with homogeneity in both scale and spread. In other words, the flow is fully dispersed. However, the flow patterns like semi-dispersed or dual continuous, the interface is sufficiently ruptured with droplets of one fluid phase into the other fluid phase are non-homogenous. With this into consideration, it is likely that the fluid phases have attained sufficient *"chaos" or turbulence* and hence, dual-continuous is evaluated using homogenous model. Employing the existing friction factor correlation of Zigrang and Sylvester (1985) but with effective Reynolds number (Re_{eff}), the homogenous model is evaluated. Accordingly, the effective friction factor for liquid-liquid flow is defined as:

$$Re_{eff} = Re_{sw} + Re_{so} \tag{13a}$$

$$\frac{1}{\sqrt{f_{eff}}} = -2 \log \left(\frac{k/D}{3.7} - \frac{4.518}{Re_{eff}} \log \left(\frac{6.9}{Re_{eff}} + \left(\frac{k/D}{3.7} \right)^{1.11} \right) \right) \tag{13b}$$

$$\frac{\Delta p}{L} = \left(\frac{f_{eff} \rho_m U_m^2}{2D} \right) \tag{13c}$$

In the literature, the mean friction factor (f_m) is determined using Eq. (5f), and by employing the mean or mixture Reynolds number (Re_m) (Eq. (5e)). The Re_m is calculated based on aggregate fluid properties like density and viscosity. Though, in the literature, it is demonstrated that the aggregate mean density ($\rho_m = \varphi_w \rho_w + \varphi_o \rho_o$) may satisfactorily characterize the flow, considerable discrepancy arise with the aggregate mean viscosity ($\mu_m = \varphi_w \mu_w + \varphi_o \mu_o$) or effective viscosity (correlations of Roscoe, 1952, Brinkman, 1952 and Pal, 1993) with φ as fluid volume fraction. In other words, these mean viscosity correlations do not characterize the viscosity of oil-water flow in general and are found to be erroneous (Hapanowicz and Polaczek, 2013; Mukhaimer et al., 2015). Such deviations in the determination of effective viscosity gets amplified when the viscosity differential between the two phases is large. For example, from the data of Dasari et al. (2014), when $U_{sw} = 0.53$ m/s and $U_{so} = 0.12$ m/s, the mean or mixture Reynolds number is found to be $Re_m = 775$ (laminar regime). In reality, the flow is not laminar. However, for the same flow conditions, the superficial Reynolds numbers of water and oil are found to be $Re_{sw} = 13{,}250$ and $Re_{so} = 25$. That is, the effective Reynolds number is $Re_{eff} = Re_{so} + Re_{sw} = 13{,}275$ (turbulent regime). Therefore, it may be reasoned that the effective Reynolds number (Re_{eff}) better represents the flow regime than the mean or mixture Reynolds number (Re_m) for wide range (from low to high) of oil viscosities.

Note that the effective friction factor correlation, Eq. (13b), is without any modification of Zigrang and Sylvester (1985). The friction factor correlation of Zigrang and Sylvester (1985) is selected since Eq. (13b), according to Zigrang and Sylvester (1985), offers a reasonable compromise between complexity and accuracy and recommended for calculation of all friction factors for turbulent flows for all roughness ratios and Reynolds numbers. Also, researchers like Angeli and Hewitt (1998), Al-Wahaibi (2012), Al-Wahaibi et al. (2007b) have employed this friction factor correlation for investigation of semi-dispersed (dual-continuous) and dispersed oil-water flow.

2.3. Experimental methods

The experiments are conducted in the multi-phase flow set-up available at C. Abdul Hakeem College of Engineering and Technology, India. The multiphase flow test rig is made up of 1.59 cm diameter stainless steel pipe of 11.25 m length with length to diameter ratio of 708 and the pipe is mounted horizontally. A schematic of experimental set-up is shown in Fig. 2. The oil and water are supplied from respective tanks. Water and oil from respective tanks are allowed to enter into the test section through a T-junction. The experimental set-up and the oil phases is same as that of employed by Ahmed and John (2021a) but for the steel pipe is extended to 11.25 m and thus may be referred for more details. The viscosity and density of oil phases are: 202, 630 mPa·s and 901, 919 kg/m^3 respectively. In the present experiments, stratified (ST), stratified wavy (SW) and dispersed (o/w and w/o) are considered (refer Fig. 4). The flow rates are assured to commensurate with the flow patterns. That is, the oil and water flow rates are in the range of 0.022–0.56 m^3/s resulting in the superficial velocity range of oil and water respectively as $0.11 < U_{so} < 2.8$ m/s and $0.11 < U_{sw} < 2.8$ m/s. For the observed flow patterns in the present experiments, the superficial velocities of oil phase and water phase are plotted in Fig. 3. Also, in Fig. 3, the superficial velocities of oil and water observed by Dasari et al. (2014) for similar flow patterns are plotted. For the stratified and stratified wavy flow patterns, no pump is used and the head of 2 m is found to be sufficient. However, for higher flow rates (dispersed flow), 0.5 hp pump is employed. The flow rates are measured using gear flow meter (accuracy ±1%) for oil and turbine flow meter (accuracy ±0.5%) for

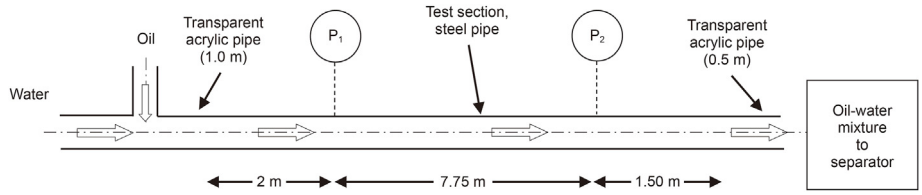

Fig. 2. Schematic illustration of experimental test setup.

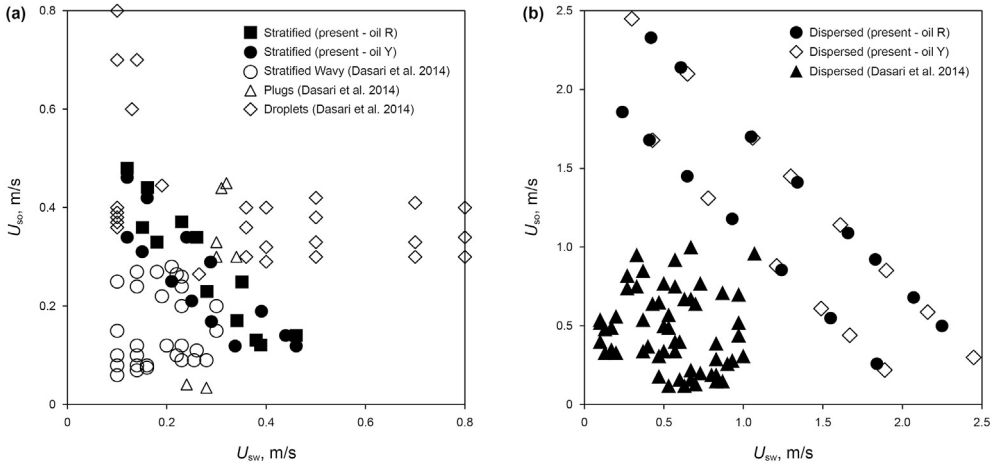

Fig. 3. The flow pattern maps of the present experimentation and Dasari et al. (2014).

water. Pressure gradient across the oil-water flow is measured using calibrated pressure transducer (Equinox make: −1 bar−3 bar with an accuracy of ±1% FS). Two pressure taps are located at 2 m and at 9.75 m from the entry resulting in 7.75 m as test section effectively. In-situ volume fraction of fluid phases are obtained using quick-closing-valve technique. Two manually controlled valves are located after the test section and 0.6 m apart. The in-situ hold-up experiments are not conducted for dispersed flow. At the end of the test section, the oil-water is allowed into tank for separation of the oil and water by gravity. The separated oil is pumped back to the respective storage tank with water discarded and fresh water is supplied to water tank. For visualization of flow patterns observed, a transparent acrylic pipe of similar diameter is attached at the entry and exit of the test section and flow patterns are captured using Nikon D3300 high speed camera. The captured images are given in Fig. 4. The stratified wavy flow patterns for oil-R and oil-Y are given in Fig. 4(a) and (b). Similarly, the oil dominated dispersed flow patterns (Dw/o-o) observed for oil-R and oil-Y are given as Fig. 4(c) and (d) and the water dominated dispersed flow (Do/w) is shown as Fig. 4(e) and (f).

Further, to determine the roughness of experimental test steel pipe, experiments are conducted using water. The procedure adapted by Angeli and Hewitt (1998) using correlation of Zigrang and Sylvester (1985) is followed. The data obtained is fitted to estimate the roughness of test section pipe and the wall roughness is found to be 7.70×10^{-5} m. There are about 54 data collected comprising different flow patterns. In addition, tests are repeated for each flow pattern to verify the repeatability. Accordingly, the uncertainties in the pressure measurements range ±8.45% for low flow rate stratified flow measurements and ±1.42% for high flow rate dispersed flow measurements with 95% confidence. The experimental uncertainty of the fluid flow rates in the present experiments are estimated to be ±1.28% with 95% confidence.

2.4. Error analysis

Further, to determine the error in the proposed correlations, Eqs. (11) and (12), for stratified flow and formulations, Eq. (13a) to Eq. (13c), average error (*AE*), absolute average error (*AAE*) and standard deviation (*SD*) of error in the pressure gradient prediction of each data set are respectively evaluated using Eq. (14a) to Eq. (14c).

$$AE = \frac{1}{n}\sum \frac{\Delta P_{exp} - \Delta P_{pre}}{\Delta P_{exp}} \times 100 \tag{14a}$$

$$AAE = \frac{1}{n}\sum \frac{\left|\Delta P_{exp} - \Delta P_{pre}\right|}{\Delta P_{exp}} \times 100 \tag{14b}$$

$$SD = \left[\sqrt{\frac{1}{n-1}\sum \left(\frac{\left|\Delta P_{exp} - \Delta P_{pre}\right|}{\Delta P_{exp}}\right)^2}\right] \times 100 \tag{14c}$$

3. Results and discussion

3.1. Stratified flow (stratified and stratified wavy)

The pressure gradient measured for various superficial oil and superficial water velocities, across the 7.75 m test section of steel pipe for stratified and stratified wavy, using high viscous oils are shown in Fig. 5(a) (oil-R) and Fig. 5(b) (oil-Y). Fig. 6(a) and (b) shows the pressure gradient variation with water mass fraction. From Figs. 5 and 6, it may be inferred that the pressure gradient decrease with increase in water mass fraction. This is similar to the observation in the literature (Nadler and Mewes, 1997; Rodriguez and

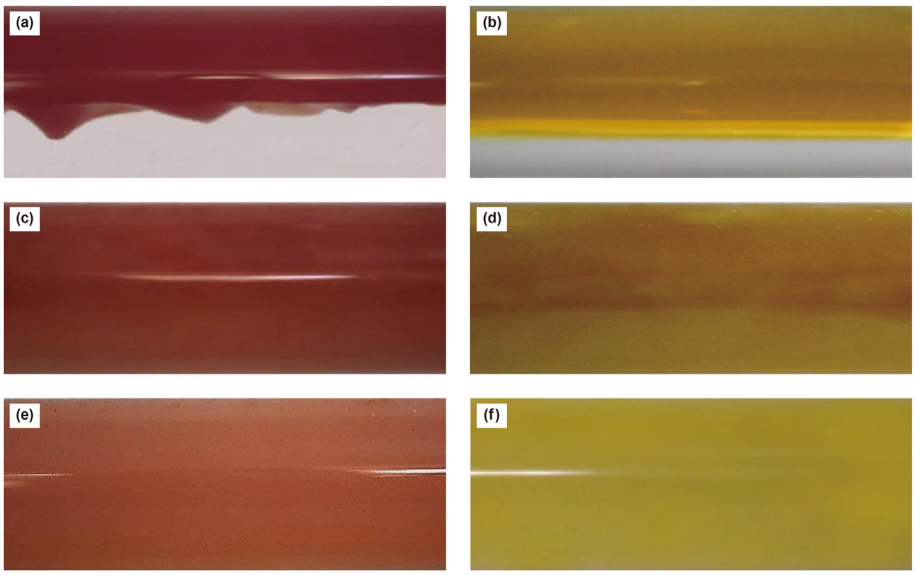

Fig. 4. Photographs of oil-water flow representing flow patterns, (**a**) and (**b**) stratified and stratified-wavy; (**c**) and (**d**) dispersed (water-in-oil/oil); (**e**) and (**f**) dispersed (oil-in-water).

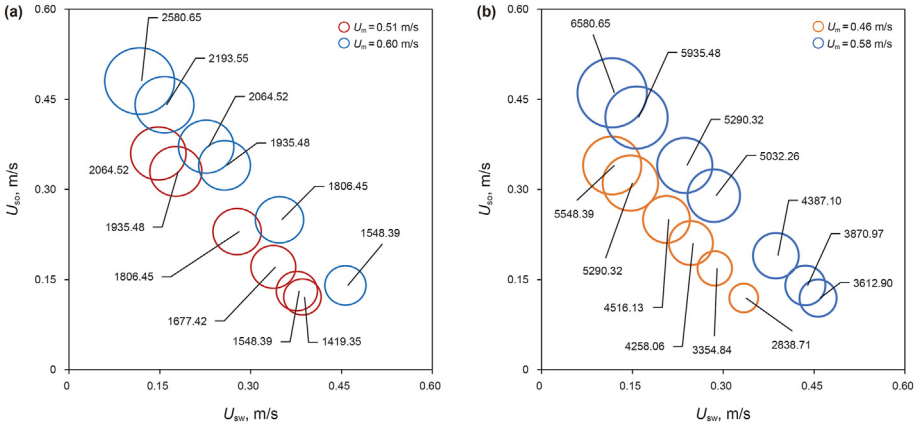

Fig. 5. Stratified flow pressure gradient (Pa/m) for various superficial velocity of oil (U_{so}) and water (U_{sw}), (**a**) oil-R and (**b**) oil-Y.

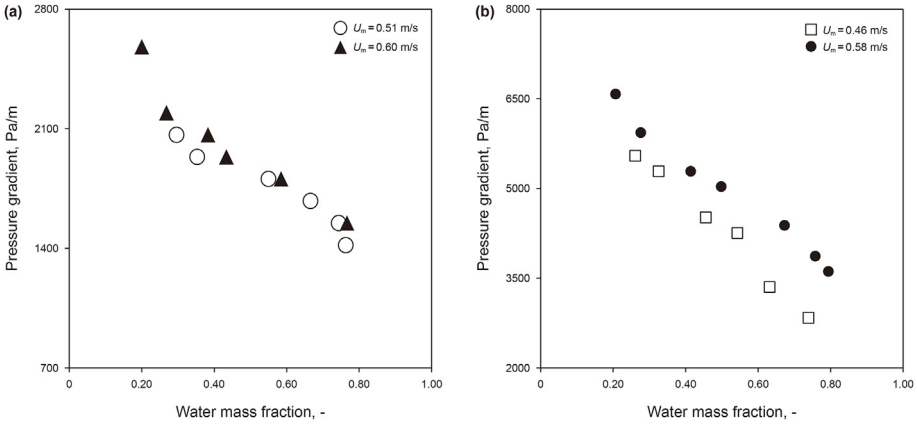

Fig. 6. Stratified flow pressure gradient (Pa/m) versus input water fraction, (**a**) oil-R and (**b**) oil-Y.

Baldani, 2012; Dasari et al., 2014), that the increase in the water mass fraction decrease the pressure gradient of moderate and high viscous oil-water flow. As noted in the previous sections, that the behavior of decreasing pressure gradient with increase of water

phase is specific to moderate and high viscous oil-water flows. Note that, for low viscous oil-water flows, the increase in water phase increases the pressure gradient (Angeli and Hewitt, 1998, Chakrabarti et al., 2005).

As described in the preceding sections, the experimental data shows that for low viscous oil-water flows ($\mu_o \approx 2$ mPa·s), the pressure gradient increases with increase of water mass fraction. In contrast, for oil viscosities >2 mPa·s, the pressure gradient decreases with water mass fraction. Based on this consideration, for the present analysis the experimental data is yet again classified as: i) data sets with viscosity of oil up to 2 mPa·s, ii) data sets with oil viscosities from 2 to 100 mPa·s, and iii) data sets with oil viscosity >100 mPa·s. This is similar to the classification as: oil phase <10 mPa·s is considered as low viscous oil, 20–100 mPa·s as medium viscous oil and >100 mPa·s as high viscous oil (Abubakar et al., 2015; Tan et al., 2018). However, note that the present classification is based on the distinctive flow behavior in relation to water phase volume fraction. Employing the friction factor correlations, Eqs. (11a) and (11b), developed using dimensional analysis (refer section 2.1) for stratified and stratified wavy (referred as S), the experimental data of stratified and stratified wavy flow pattern obtained from the literature is analyzed. Here, note that Edomwonyi-Otu and Angeli (2014) evaluates the two-fluid model with experimental data of stratified (separated) regions: stratified, stratified wavy and rivulet. Accordingly, rivulet flow pattern data is also included in the analysis as stratified. For the analysis of Eqs. (11a) and (11b), the values of contact angles for different pipe materials are based on the recommendations by Rodriguez and Baldani (2012). The wetting angles of 60° for steel, 110° for acrylic and 30° for glass are considered, unless specified in the respective research work. Since the experimental data using glass pipe is only of Rodriguez and Baldani (2012) and Bochio et al. (2021), the contact angle (30°) observed by Rodriguez and Baldani (2012) is employed in the present analysis. The multivariate regression technique is employed. Accordingly, from regression analysis, the constant (A) and exponents (a, b, c and d) of the friction factor equations, Eqs. (11a) and (11b), are determined and indicated in Table 2. The experimental data of Elseth (2001), Al-Wahaibi et al. (2007b), Bochio et al. (2021) and the present experiments are considered as test data and hence not included in the regression

3.1.1. Effect of viscosity ratio

From the regression analysis, the viscosity ratio is found to significantly enhance the prediction of pressure gradient for moderate viscosity oil-water flows but not for the low and high viscous oil-water flows. For low viscous oil-water flows range only (refer Table 1) from 1.2 mPa·s (Chakrabarti et al., 2005)–1.64 mPa·s (Elseth, 2001). This behavior is expected for low viscous oil-water flow. Since the viscosity of oil and water are comparable, the attainment of turbulence (boundary layer characteristics) in both fluid phases would be almost concurrent. Further, as there is sufficient evidence on the effect of viscosity, it is evident for moderate viscous oil-water flow. Here, note that the available viscosity range is from 2 to 100 mPa·s and the experimental data available range from 3.5 (Liu et al., 2008)–29 mPa·s (Trallero et al., 1997). There is no data available with viscosity ratio ranging from 29 to 100. With more experimental data in this range (29–100 mPa·s), friction factor may further be enhanced. Interestingly, though it is highly probable that there is significant effect of viscosity of oil on friction factor, the analysis shows the contrary. This could possibly due to the very narrow range of oil viscosity considered for analysis (107 mPa·s (Dasari et al., 2014), 280 mPa·s (Rodriguez and Baldani, 2012), 202 and 630 mPa·s of the present work).

3.1.2. Effect of superficial velocities and superficial Reynolds number of fluid phases

The exponent values of superficial Reynolds number range from −0.15 to −0.93 across the entire range of oil viscosity considered. Interestingly, these values are approaching to the exponent values of Blausius equation ($m = -0.2$ for turbulent and $m = -1$ for laminar in equation $f = CRe^m$). Note that, for low viscous oil-water flows, the superficial Reynolds number exponents are −0.193 and −0.151 for water and oil respectively. Here, note that the contribution of both oil and water phase to the pressure gradient almost equally for low (<2 mPa·s). For moderate (2–100 mPa·s) viscous oil-water flow, the superficial Reynolds number exponent values observed are −0.813 and −0.675 for water and oil respectively. Incidentally, these values are nearer to the single phase laminar flow friction factor Reynolds number exponent of −1. Also, for both low viscous and moderate viscous oil-water flows, note that the water superficial Reynolds number value contributes lesser than that of oil superficial Reynolds number. However, for moderate viscous oil, the exponent values for water superficial Reynolds number are higher than that of low viscous oil-water flow. Possibly, due to the acceleration of water fluid phase. Here, it may recalled that, for moderate and high viscous oils, the water phase accelerate compared to that of oil phase indicated by their hold-up values (Trallero et al., 1997; Rodriguez and Baldani, 2012; Edomwonyi-Otu and Angeli, 2014). Further, in contrast, for high viscous (>100 mPa·s) oil-water flows, the water phase superficial Reynolds number value is much greater than that of the oil phase superficial Reynolds number value. Note that the oil phase remains laminar for much higher flow rates compared to that of low and moderate viscous oil-water flows.

3.1.3. Effect of wetting angle

Representing the interfacial curvature, the effect of contact/wetting angle on the pressure gradient may be noted. The

Table 2
Constants in friction factor equations, Eqs. (11a) and (11b).

S.No	Viscosity, Pa·s	Fluid phase friction factor	a (Re_{sf})	b (θ_c)	c (ε_w)	d $\left(\frac{\mu_o}{\mu_w}\right)$	A (constant)
1.	0.001 – 0.002	f_w	−0.193	−0.778	0.252	−0.012	0.067
		f_o	−0.151	−0.791	−0.075	−0.207	0.032
2.	0.002 – 0.10	f_w	−0.813	−1.095	0.672	0.813	1.68
		f_o	−0.675	−1.142	−0.595	0.062	0.355
3.	>0.1	f_w	−0.161	−0.381	−0.324	0	1786.44
		f_o	−0.934	0.029	−1.327	0	0.385

dimensionless contact angle term for low viscous oil-water flow (with exponential value of: −0.753 for water phase and −0.791 for oil phase), effectively contributes higher for steel pipe (wetting angle ratio: $\theta_c = 0.67$) compared with the acrylic pipe (wetting angle ratio: $\theta_c = 1.22$). Consequently, the higher pressure gradient for the steel pipe than that of acrylic pipe is observed which conforms to the experimental observation. Similar to the observation for low oil-water flow, the wetting angle term affects the friction factors of moderate and high viscous oil-water flows. Further, it may be emphasized that the contact (wetting angles) suggested in the literature are measured under static condition and hence, the dynamic contact angle may differ (Rodriguez and Baldani, 2012). The contact/wetting angle also dependent on the pipe material being pre-wetted with either oil or water phase (Angeli and Hewitt, 1998). However, the wetting angles are rarely measured in the literature and are generally not available with the oil-water pressure gradient investigations.

3.1.4. Effect of fluid phase fraction

The water fraction is found to affect the moderate and high viscous oil-water flow significantly. For high viscous oil-water flow with high oil phase fraction, the effect of oil phase friction factor is found to be substantially high. Similarly, for moderate viscous oil-water flow (2–100 mPa•s), the increase of water fraction decrease the pressure gradient. Note that the phenomenon is similar in both moderate and high viscous oil-water but on lesser magnitude compared to high viscous oil. However, for the experimental data with low viscosity <2 mPa•s, the effect of water fraction on the friction factor or pressure gradient is not very significant.

Applying these friction factor correlations (Eq. (11)) in two-fluid model, Fig. 7 shows the experimental pressure gradient and the predicted pressure gradient for the data (including present experiments) listed in Table 1. A 20% error line is also indicated. Details of average error, absolute average error and standard deviation in the prediction of pressure gradient of each data set calculated using equations, Eqs. (11) and (12) are given in Table 3. The prediction is improved for all data sets with 90% of experimental data is predicted within ±30% and 75% of the experimental data is predicted within ±20%. Though the prediction of the data of Bochio et al. (2021) is improved using the proposed correlation, yet the prediction error is in range of ≈70%.

According to Oliemans (2011), average errors in the range of 20%–40% and with maximum error exceeding 100% are common. However, the prediction using the proposed correlations results in average range of errors are substantially reduced to 5%–25% with maximum error in the order of 60%. Notably, the high errors of ≈200% (Chakrabarti et al., 2005) at low volume fractions (Rodriguez et al., 2012) observed in the literature are not found. Note that Rodriguez et al. (2012) observed that the high errors systematically observed at low volume fraction may not be attributed to experimental uncertainties but on the closure relations. Nevertheless, using the proposed correlations, the maximum error (≈60%) observed are not specific to low volume fraction rather random. Further, for the experimental data of (Bochio et al., 2021) using high viscous oil-water flow through glass pipe indicates high percentage of error. Here, unlike the experimental data with acrylic pipes is available in the range 0.0016–0.06 Pa•s, the experimental data with pipes of other materials (like steel and glass) is very limited. That is, Angeli and Hewitt (1998), Rodriguez and Oliemans (2006) and Liu et al. (2008) for steel and Rodriguez and Baldani (2012) and Bochio et al. (2021) for glass. Therefore, further experimental data of oil-water flow in steel and glass pipe may facilitate improved comprehension of the characteristics of pressure gradient employing these dimensionless parameters.

Of the exclusive stratified flow 15 data sets and 195 data points considered for evaluation, the average percentage error (*AE*) is 8.12% and the absolute average percentage error (*MAE*) is 15.27% with a standard deviation (*SD*) of 20.52%. This may be considered to be satisfactorily when compared with the prediction using the existing friction factor correlations. Except the data set of Bochio et al. (2021), wherein the respective values are: *AE* is 51.62% and with a *SD* of 71.65%. From the above Table 3, the prediction employing the proposed correlation, the error percentages of all the data sets considered for evaluation are improved, except the data sets of Nadler and Mewes (1997) and Angeli and Hewitt (1998) (acrylic). The two-fluid model using the existing wall and interfacial correlation indicate high percentage errors in predicting pressure gradient.

In summary, the critical parameters effecting the pressure gradient of oil-water stratified flows are therefore incorporated into the proposed friction factor correlations. That is, i) the wall or boundary effects and viscosity effects using superficial Reynolds number, ii) the effect of interfacial curvature (or pipe material) using contact/wetting angle and iii) the effect of fluid volume fraction. The analysis employing the proposed friction factor correlations into the two-fluid model indicates satisfactory prediction of pressure gradient with reduced average error and standard deviation than that of conventional/existing correlations in the literature.

3.2. Dual-continuous to dispersed (D) flow patterns

The pressure gradient measured for dispersed flow pattern is plotted in Figs. 8 and 9 for superficial fluid velocities and water mass fractions. The pressure gradient gradually increases with the increase of oil phase. When the dispersion is non-homogeneous, interestingly, an oil dominated flow structure is observed slightly away from the upper wall and this space is occupied with water dominated flow (Fig. 4(c) and (d)). In other words, water droplets are found near the upper wall and similar phenomenon was also indicated by Rodriguez et al. (2012). With further increase of flow velocity, homogeneous dispersion of oil in water with oil uniformly dispersed across the pipe cross-section. Such homogeneous dispersed flow is observed only at low oil volume fractions due to high viscous oil phase. Further, there is possibility of phase inversion phenomenon occurring while the continuous fluid phase changes from water to oil and vice versa similar to that of observed by Pal (1993). In the present experiments, however the phase inversion phenomenon or abrupt pressure gradient may not be inferred from the experimental data due to the lack of instrumentation to verify the homogeneity and continuous fluid phase. Therefore, exact phase inversion cannot be identified. Here, it may also be noted that the extent of pressure gradient change observed by Pal (1993) is rarely observed in the literature of oil-water flow. For example, Trallero et al. (1997) do not observed the phase inversion, likely due to high flow rates. Nadler and Mewes (1997) and Yusuf et al. (2012) indicates phase inversion but the change in pressure gradient is nominal. The abrupt increase of Pal (1993) may be due to the flow conditions. That is, Pal and Rhodes (1989) employed stirring of oil and water prior to the entry into the pipe, which is not the case with the experiments considered in the present work. Though pumps are employed to generate required flow rate, stirring of oil and water prior to entry is not considered.

For dual-continuous to fully dispersed flow patterns, the existing homogenous model is employed with effective Reynolds number (Eq. (13a)) and the friction factor correlation of Zigrang and Sylvester (1985). As discussed in the preceding section 2.1, the effective Reynolds number is defined as the sum of superficial Reynolds number of oil and superficial Reynolds number of water.

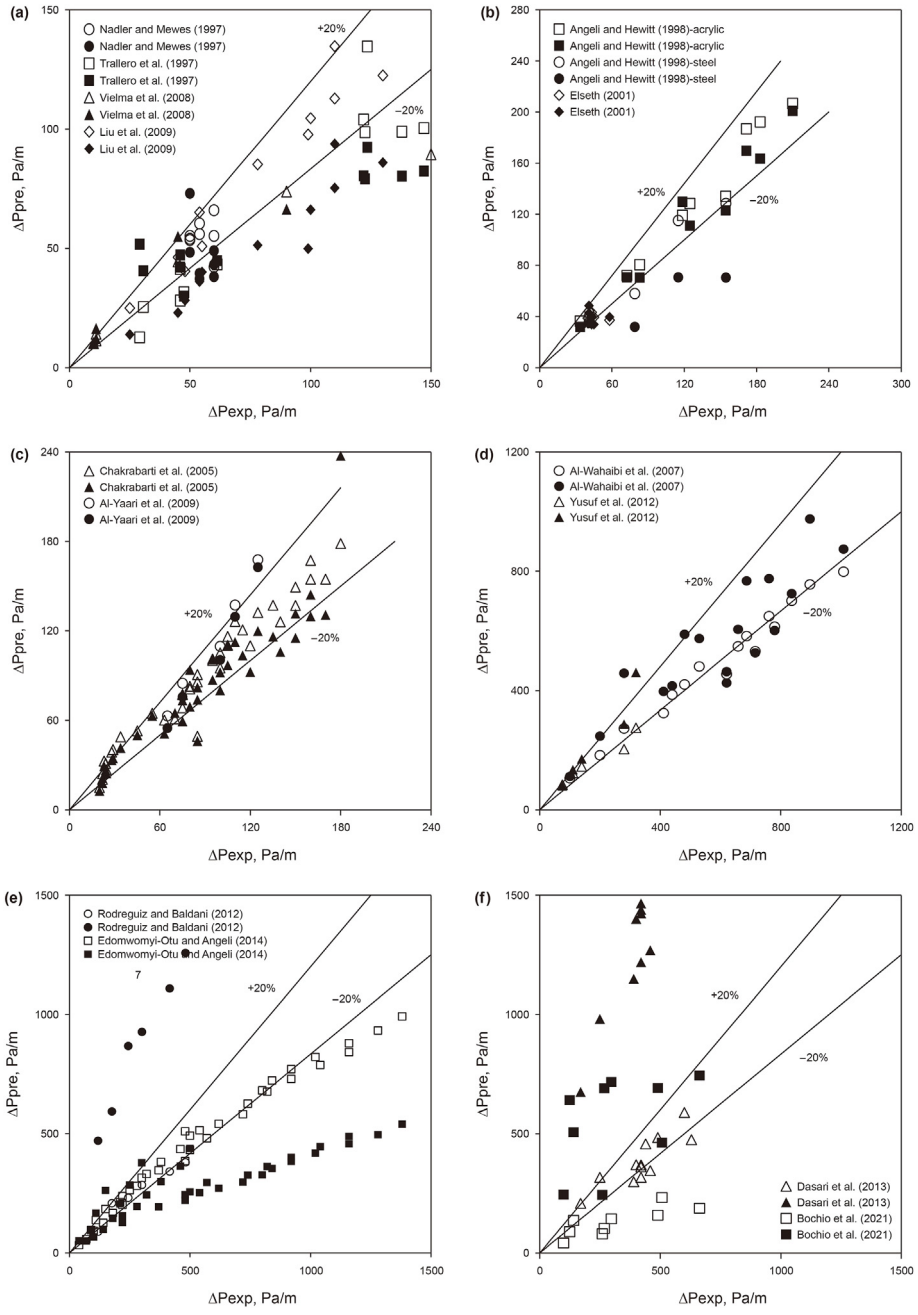

Fig. 7. Stratified flow: experimental versus predicted pressure gradient. (hollow symbols – proposed friction factor and shear stress correlations, Eq. (11) and Eq. (12); filled symbols – friction factor correlation existing in literature, Eq. (4a) to Eq. (4c).

In the friction factor correlation, the pipe roughness for steel, acrylic and glass of 7×10^{-5}, 1×10^{-5} and 1×10^{-6} m respectively are considered, unless specified for the respective experimental data like that of Rodriguez and Oliemans (2006) with a pipe roughness of 4.5×10^{-5} m. The experimental data from the literature (Table 1) and the data from the present experiments are analyzed. For the experimental pressure gradient data versus the predicted pressure gradient data is plotted in Fig. 10.

In general, for dispersed flow, the fluid in contact with the wall is considered significant for the pressure gradient across the flow. However, the effect of water phase in the oil-water flow system depend on the oil phase viscosity. For example, for low viscous oil-water flow of Angeli and Hewitt (1998), in both steel and acrylic pipes, Angeli and Hewitt (1998) found the water continuous dispersed flow has higher pressure gradient than that of oil continuous dispersed flow. In contrast, for moderate and high viscous oils, the pressure gradient is higher in oil dominated flow than that of water dominated flow which is similar to the observation by Rodriguez et al. (2012), Dasari et al. (2014) and also the present experiments. This decrease in pressure gradient with water phase, researchers (Lovick and Angeli, 2004; Yusuf et al., 2012) attribute as the drag reduction phenomenon.

While studying the drag reduction phenomenon, Rodriguez et al. (2012) and Abubakar et al. (2016) indicated that the formation of water sublayer near the wall is responsible for the reduction in pressure gradient for low oil phase fractions. Rodriguez et al.

Table 3
Assessment of pressure gradient correlations (stratified and stratified wavy flow).

Author	Two-fluid model (Eq. (3))								No of data points
	Using proposed friction factor correlations (Eqs. (3a), (11) and (12))				Existing friction factor correlations (Eqs. (3a), (4a) to Eq. (4e)				
	AE, %	*AE*, %	*SD*, %	Max, %	*AE*, %	*AAE*, %	*SD*, %	Max, %	
Trallero et al. (1997)	24.5	26.13	29.38	56.22	12.62	35.19	39.44	−77.83	11
Nadler and Mewes (1997)	−1.72	11.07	13.00	29.51	−54.67	90.56	191.00	−534.88	8
Angeli and Hewitt (1998) (steel)	14.68	14.68	18.38	26.89	50.90	50.90	51.68	59.64	3
Angeli and Hewitt (1998) (acrylic)	−0.73	4.84	6.37	13.32	6.78	8.86	10.68	20.51	9
Elseth (2001)	7.93	10.00	14.72	36.29	11.81	17.24	19.00	24.80	8
Chakrabarti et al. (2005)	−2.88	12.43	17.17	43.73	5.93	14.34	17.40	45.71	45
Al-Wahaibi et al. (2007b)	13.55	14.16	16.63	26.66	0.57	17.61	24.90	−63.71	18
Vielma et al. (2008)	5.53	14.26	19.70	40.33	−11.59	20.34	25.16	−48.82	6
Liu et al. (2008)	−2.91	8.46	11.00	−22.58	30.18	30.18	34.00	49.64	11
Al-Yaari et al. (2009)	−15.70	16.98	20.29	34.19	−6.72	12.98	17.15	−30.18	5
Rodriguez and Baldani (2012)	9.29	15.41	17.10	24.33	−220.77	220.77	225.97	−296.85	6
Yusuf et al. (2012)	2.43	14.04	15.92	27.13	−19.49	19.49	24.36	−43.98	5
Edomwonyi-Otu and Angeli (2014)	8.64	13.15	15.50	27.35	31.70	41.28	44.57	61.24	38
Dasari et al. (2014)	6.59	18.29	19.95	−30.76	−274.64	274.64	286.83	−515.27	14
Bochio et al. (2021)	51.62	51.62	55.78	71.65	−129.06	132.48	185.59	−417.25	9
Present - R	27.53	28.07	30.21	42.48	−356.1	356.1	429.5	−816.92	12
Present - Y	12.82	23.48	25.84	−49.04	−538.2	538.17	657.07	−1425	13

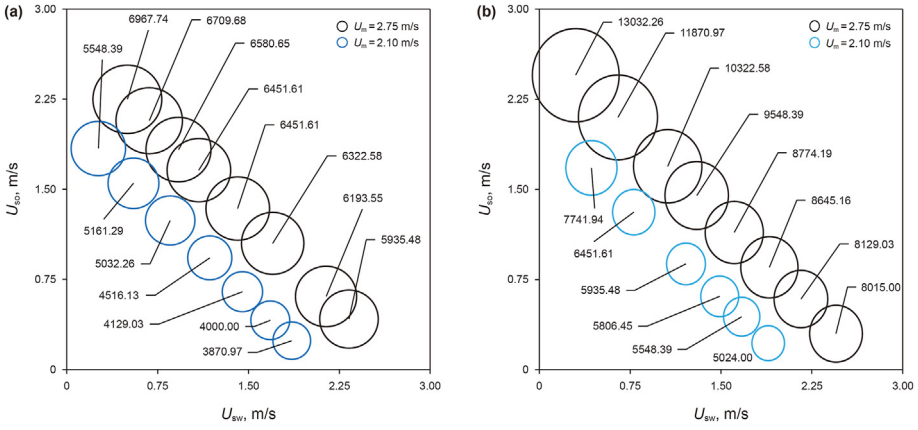

Fig. 8. Dispersed flow pressure gradient (Pa/m) for various superficial velocity of oil (U_{so}) and water (U_{sw}), (**a**) oil-R and (**b**) oil-Y.

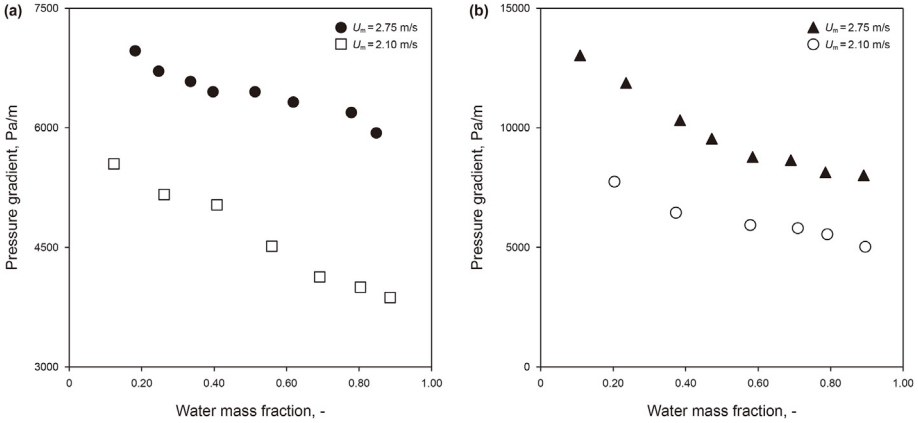

Fig. 9. Pressure gradient (Pa/m) versus input water fraction, (**a**) oil-R and (**b**) oil-Y.

(2012) noted that with increasing the water-film thickness results in low wall shear stress and hence high drag reduction. However, rather than simple presence of water phase at the pipe periphery as the reason for the drag reduction, the state of the boundary layer (laminar or turbulent) may describe for tangible drag reduction effect. As mentioned above, for Angeli and Hewitt (1998), for both water continuous and oil continuous dispersed (homogenous and non-homogenous), the pressure gradient increases with water

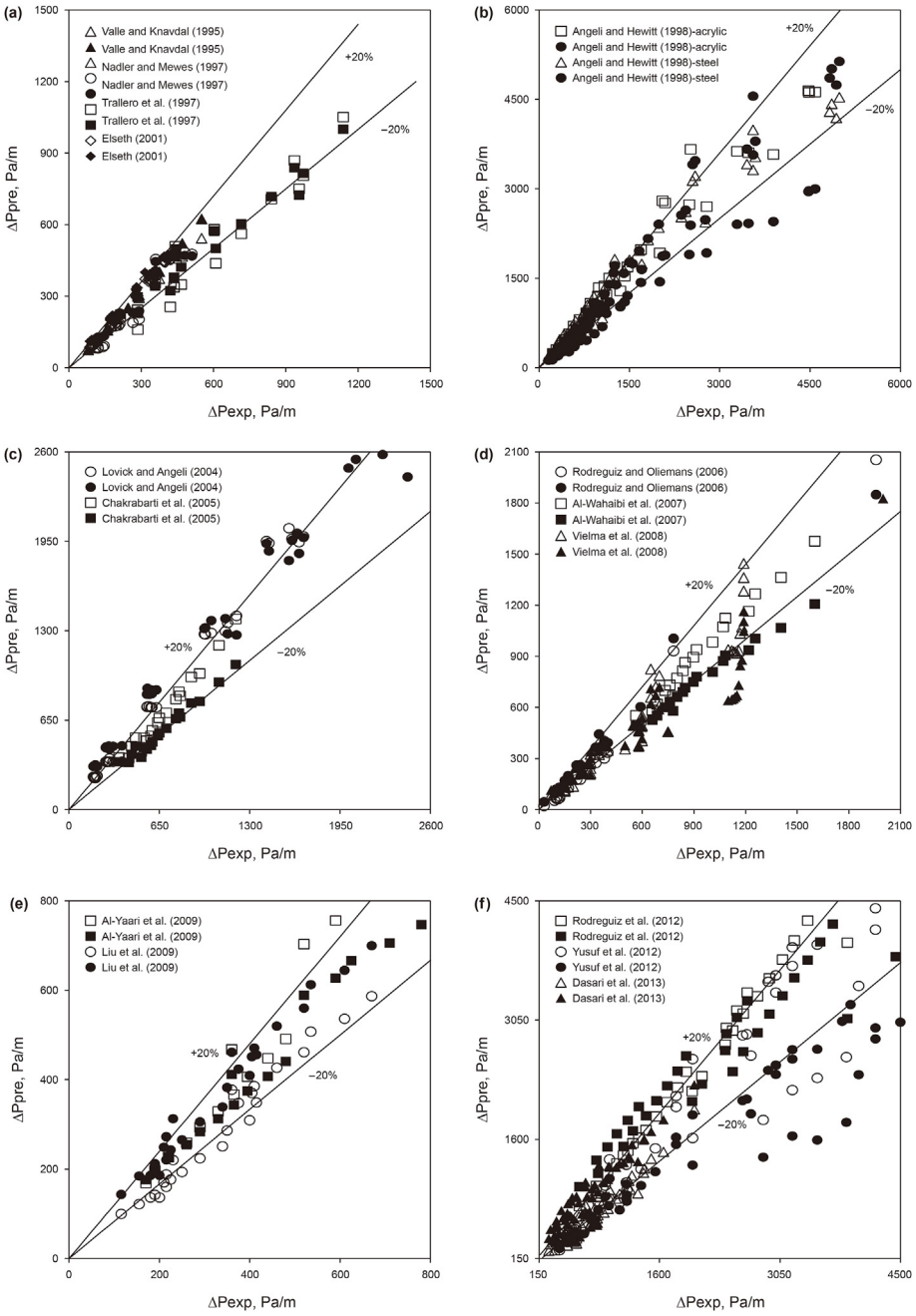

Fig. 10. Dispersed flow: experimental versus predicted pressure gradient for various data sets (hollow symbols – proposed correlation, Eq. (13a) to Eq. (13c); filled symbols – Al-Wahaibi (2012) correlation, Eq. (6a) and Eq. (6b)).

volume fraction but with a dip in pressure gradient at phase-inversion. With the drastic decrease, at phase-inversion from oil-continuous to water continuous, at water volume fraction of 30%–40%, the pressure gradient tend to remain same or increase slightly with water volume fraction (Angeli and Hewitt, 1998). That is, no drag reduction is observed with higher water phase at the periphery of the wall after phase-inversion. Further, for moderate and high viscous oils (Dasari et al., 2014; Rodriguez et al., 2012), due to oil phase viscosity, it is likely that the wall originated turbulence in water continuous flow is established much ahead compared with the oil continuous flow. Consequently, for low viscous oil-water flows, the boundary layer transition from laminar to turbulent occurs at almost similar time scale irrespective of the flow is oil continuous or water continuous. However, for moderate and high viscous oil-water continuous flows, the boundary layer transition of water phase at the periphery always precedes the boundary layer transition of oil phase at the periphery. Accordingly, for high viscous oil-water flow with water phase at the periphery, the pressure gradient is lower than that of high viscous oil-water flow with oil phase at the periphery. When the boundary layer of water phase in contact with the pipe wall becomes turbulent, it is irrelevant whether the flow is either homogenous or non-homogenous. Hence, it may be inferred that the characteristics of the boundary layer is significant for the pressure gradient reduction, rather than the particular fluid phase presence at the wall. Significantly, it should be noted that the water phase at the wall may either be due

to the hydrophilic nature of pipe or high mass flow rates of water phase (continuous phase). That is, when the pipe is of steel and glass (both are hydrophilic), the water phase likely to wet and occupy the pipe wall.

There are 527 data points from 16 literature experimental data sets that are investigated for dispersed flow. From Table 4, it is observed that the average percentage error (*AE*) is 0.31% and the absolute average percentage error (*MAE*) is 15.45% with a standard deviation (*SD*) of 18.79%. When compared with Al-Wahaibi (2012) correlation: the average error, mean absolute error and standard deviation percentages are −3.28%, 20.55% and 26.33% respectively. The maximum error percentage for each data set is also indicated. Therefore, it may be inferred that the prediction employing the proposed correlation, the error percentages of the data sets (Elseth, 2001, Lovick and Angeli, 2004, Chakrabarti et al., 2005, Al-Wahaibi et al., 2007b, Vielma et al., 2008, Rodriguez et al., 2012).

Yusuf et al. (2012) and Dasari et al. (2014) are found to be improved. However, the data sets of Valle and Kvandal (1995), Trallero et al. (1997), Angeli and Hewitt (1998), Rodriguez and Oliemans (2006) and Al-Yaari et al. (2009) have indicated higher errors with the proposed correlation than that of Al-Wahaibi (2012) correlation.

3.3. Von-Kármán constant and effective viscosity

In the preceding sections, it is satisfactorily demonstrated that the existing friction factor correlations incorporated with effective Reynolds number (Re_{eff}) predict the pressure gradient of oil-water dispersed flow. Accordingly, it may be inferred that the effective Reynolds number designate the flow system, may it be considered that the effective viscosity (μ_{eff}) of the oil-water flow from the effective Reynolds number ($Re_{\text{eff}} = Re_{\text{so}} + Re_{\text{sw}} = \frac{\rho_m U_m D}{\mu_{\text{eff}}}$). Nevertheless, the verification of the proposed definition of the effective viscosity (μ_{eff}) requires wall characteristics data. In the present work, no such wall characteristics are measured. Therefore, the von-Kármán factor (κ) is determined using the (Richardson, 1989) equation for turbulent flow (Eq. (15)). Angeli and Hewitt (1998) noted that the von Kármán factor given in Eq. (15) is appropriate for both smooth and rough pipes.

$$\sqrt{\frac{8}{f_{\text{eff}}}} = \frac{1}{\kappa}\left[\ln\left(\frac{Re_{\text{eff}}\sqrt{f_{\text{eff}}/4}}{1.0 + 0.1\left(k/D\right)Re_{\text{eff}}\sqrt{f_{\text{eff}}}}\right) - 2.54\right] + 5.35 \tag{15}$$

where f_{eff}, κ, Re_{eff}, k and D are the effective friction factor, the Von Kármán factor, the effective Reynolds number, wall roughness and the pipe diameter. Accordingly, in Eq. (15), the oil-water flow parameters are considered and the Von-Kármán factor (κ) is calculated for all data sets considered in the present work and the results are shown in Fig. 11. Interestingly, employing the proposed methodology of using effective Reynolds number in the existing friction factor correlations results in Von-Kármán factor of almost ≈0.4 for all data sets and data points. Except that the Dasari et al. (2014) indicates deviation up to 0.8. With the correlation of Al-Wahaibi (2012), the Von-Kármán factor vary significantly, particularly indicate much higher values than 0.4. Here, in the literature of turbulence, for the flow to be considered to have attained turbulence, the experimental values of the Von Kármán constant are in the range of 0.36–0.37 (Telford and Businger, 1986), 0.40–0.41 (Hinze, 1975) and the large eddy simulation result of 0.35–0.36 (Cai and Steyn, 1996). Therefore, it may be inferred that the effective friction factor determined using the effective Reynolds number describe the turbulence characteristics of dispersed oil-water flow system.

3.4. Fluid hold-up analysis

The in-situ fluid volume fractions of stratified flow (stratified and stratified wavy) measured by the quick-closing-valve technique are analyzed and compared with the prediction using the two-fluid model (Eq. (3b)) and proposed interfacial closure relations (Eq. (12c)). In the literature, it is established fact that, for moderate and high viscous oil-water flows, the acceleration of water phase with respect to that of oil phase affects the hold-up fraction (Trallero et al., 1997; Rodriguez and Baldani, 2012; Edomwonyi-Otu and Angeli, 2014). Therefore, in the prediction of hold-up, the effect of viscosity of oil phase, the interfacial curvature (contact/wetting angle) and the fluid phase fraction are included.

Table 4
Assessment of pressure gradient correlations (dual-continuous and dispersed flow).

Author(s)	Proposed methodology (Eqs. (13a), (13b) and (13c))				Al-Wahaibi (2012) correlation (Eqs. (6a) and (6b))				No of data points
	AE, %	*AAE*, %	*SD*, %	Max, %	*AE*, %	*AAE*, %	*SD*, %	Max, %	
Valle and Kvandal (1995)	3.51	6.61	7.58	13.32	2.49	3.03	4.09	10.19	10
Nadler and Mewes (1997)	−16.31	21.41	24.23	−39.95	2.15	9.89	11.09	23.61	16
Trallero et al. (1997)	−14.52	16.50	20.27	−44.04	−8.55	11.76	13.29	−37.07	20
Angeli and Hewitt (1998) (steel)	−3.32	18.07	22.59	−46.81	7.31	16.57	19.38	44.37	62
Angeli and Hewitt (1998) (acrylic)	8.20	12.86	16.72	45.42	−14.33	14.44	17.87	−37.07	43
Elseth (2001)	3.45	6.21	7.39	18.06	19.23	19.23	19.64	29.16	43
Lovick and Angeli (2004)	23.87	24.23	25.25	37.33	41.23	41.26	47.39	77.61	45
Chakrabarti et al. (2005)	9.23	7.08	8.60	−18.67	−14.89	14.89	15.87	−26.79	19
Rodriguez and Oliemans (2006)	22.39	24.77	27.56	44.54	−11.26	13.22	17.38	−26.45	20
Al-Wahaibi et al. (2007b)	−3.16	4.13	5.64	−11.46	19.08	19.08	19.39	−24.69	18
Vielma et al. (2008)	−11.30	17.59	19.79	−39.22	−13.14	17.92	23.23	62.63	46
Liu et al. (2008)	−15.72	16.40	17.90	−31.82	11.51	12.09	15.00	35.84	25
Al-Yaari et al. (2009)	10.98	11.17	16.73	35.20	0.45	6.25	7.25	14.32	17
Rodriguez et al. (2012)	13.07	13.41	14.50	20.79	21.34	24.13	30.02	29.66	33
Yusuf et al. (2012)	−5.97	18.39	20.94	−36.78	−26.41	26.92	30.33	−56.70	49
Dasari et al. (2014)	−12.05	14.13	17.77	−44.86	21.31	29.54	35.03	73.98	61
Present - R	13.04	14.95	17.12	27.95	26.47	26.47	27.45	35.41	15
Present - Y	20.17	20.17	21.54	32.95	12.48	13.88	15.64	27.06	14

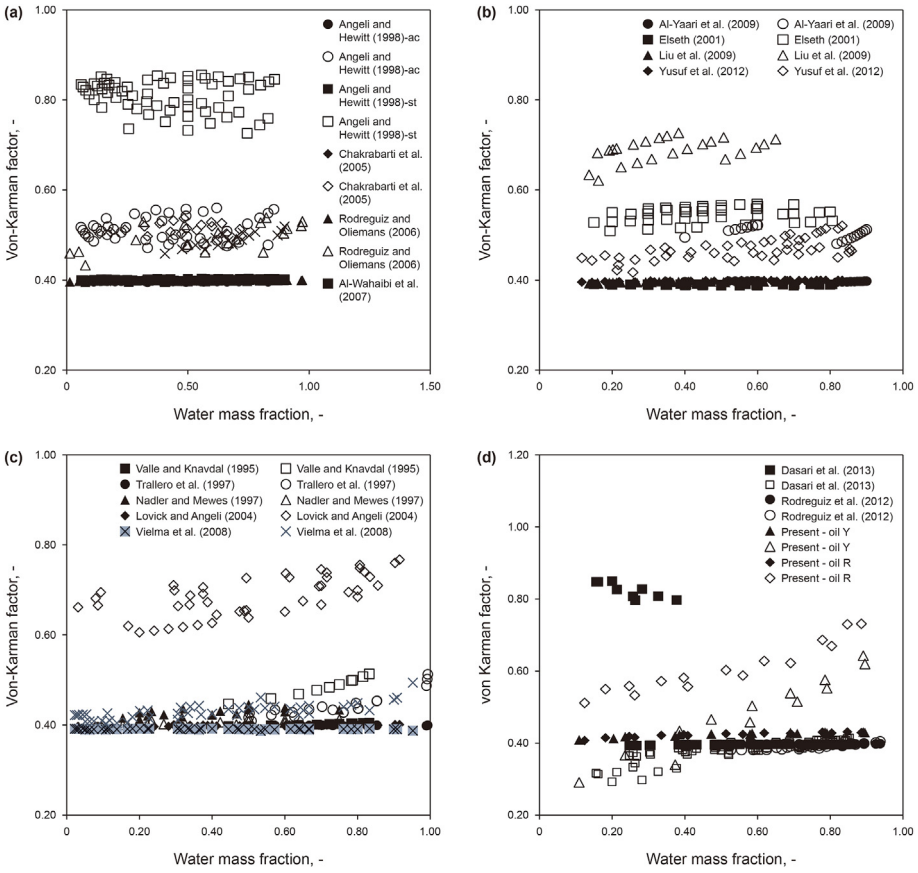

Fig. 11. Von-Kármán factor (filled symbols - proposed correlation, Eq. (13); hollow symbols – Al-Wahaibi (2012) correlation, Eq. (6a) and Eq. (6b).

The representation of fluid velocities using superficial velocities and fluid phase Reynolds number, specifically at low volume fluid fraction, into the two-fluid model equations improved the prediction of hold-up fraction substantially. Further, since the closure equation of the interface should describe the mutual interaction of both fluid phases at the interface (Liu et al., 2008; Clausse and de Bertodano, 2021), the proposed interfacial relation (Eq. (12c)) designates the interaction of the momentum of the two fluid phases at the interface. Hence, replacement of the fluid velocities in the interfacial relation with superficial fluid velocities, substantial reduction in the hold-up error is observed (Table 5). For the data of Trallero et al. (1997), the hold-up volume fraction prediction error observed using conventional closure relations is in the range of 50% which substantially reduced to approximately 20% using the proposed closure correlations. Similarly, the data of Rodriguez and Baldani (2012) indicates an error exceeding 200% using conventional correlations compared to 10% with that of proposed correlations. There is substantial improvement in the prediction of in-situ hold-up volume fraction using Eq. (11a) to Eq. (11b) and Eq. (12a) to Eq. (12c) compared to that of conventional closure relations, Eq. (4a) to Eq. (4e).

4. Conclusions

From the investigation of pressure gradient and hold up experimental data, the important inferences are as follows. The 19 experimental data sets from the literature and the present experiments consisting of wide range of fluid properties

Table 5
Assessment of hold-up fraction (stratified and stratified wavy flow - S).

Author(s)	Two-fluid model, Eq. (3)						No of data points
	Using proposed friction factor correlation, Eq. (12)			Existing oil-water flow friction factor correlations, Eq. (4a) to Eq. (4d)			
	AE, %	*SD*, %	Max., %	*AE*, %	*SD*, %	Max., %	
Trallero et al. (1997)	9.00	10.00	25.00	4.00	20.00	44.00	9
Elseth (2001)	1.02	15.05	16.40	−9.46	15.05	−36.37	3
Vielma et al. (2008)	6.80	9.40	23.70	9.40	29.40	67.50	19
Liu et al. (2008)	9.80	10.20	13.60	15.80	39.08	52.10	5
Rodriguez and Baldani (2012)	−0.19	12.39	15.83	90.69	3.14	94.71	6
Edomwonyi-Otu and Angeli (2014)	9.00	8.00	25.00	4.00	29.00	−81.00	29
Present - R	6.68	24.07	75.36	91.44	7.53	98.45	12
Present - Y	−4.26	27.07	−71.96	96.75	2.32	99.17	13

(0.00164–0.630 Pa•s) are classified into: i) low viscous oil-water flow (≈2 mPa•s), ii) moderate viscous oil-water flow (2–100 mPa•s) and iii) high viscous oil-water flow (>100 mPa•s). For the analysis, the oil-water pipe flow is evaluated segregating into two categories of flow patterns as i) stratified - consisting of stratified and stratified wavy flow patterns and ii) remaining flow patterns with interfacial droplets, dual-continuous and fully dispersed as dispersed. The stratified flow is analyzed using two-fluid model and dispersed flow using the homogenous model.

The effects of viscosity, the interfacial curvature (using contact/wetting angle) and the fluid volume fraction are incorporated into the friction factor correlation through dimensional analysis. The primary cause of high percentages of errors in stratified flow is the misrepresentation of fluid phase velocities using calculated fluid phase velocities (U_o and U_w). The wall (τ_w and τ_o) and interfacial stress (τ_i) equations are modified employing the superficial fluid velocities and the proposed friction factor correlations. The superficial Reynolds numbers (Re_{sw} and Re_{so}) and not the fluid phase Reynolds numbers (Re_w and Re_o) are employed in the analysis. Employing the proposed friction factor and wall and interfacial stress correlations, the prediction of pressure gradient of oil-water flow and the fluid hold-up fraction is found to be enhanced. For dispersed flow, an effective Reynolds number (Re_{eff}) is defined as summation of superficial Reynolds number of oil and water phase. Employing the effective Reynolds number, the existing single phase turbulent friction factor correlation predicts the pressure gradient of oil-water dispersed flow satisfactorily. The percentage error and standard deviation in the prediction, for both stratified and dispersed flow, are substantially reduced. The proposed correlations may further be improved with more experimental data with high viscous oils and different pipe materials. Since, the data available in the literature for high viscous stratified oil-water flow is meagre.

Conflict of interest

We wish to confirm that there are no known conflicts of interest associated with this publication and there has been no significant financial support for this work that could have influenced its outcome.

References

Abubakar, A., Al-Wahaibi, Y., Al-Wahaibi, T., Al-Hashmi, A., Al-Ajmi, A., Eshrati, M., 2015. Effect of low interfacial tension on flow patterns, pressure gradients and holdups of medium-viscosity oil/water flow in horizontal pipe. Exp. Therm. Fluid Sci. 68, 58–67. https://doi.org/10.1016/j.expthermflusci.2015.02.017.

Abubakar, A., Al-Wahaibi, T., Al-Hashmi, A., Al-Wahaibi, Y., Al-Ajmi, A., Eshrati, M., 2016. Empirical correlation for predicting pressure gradients of oil-water flow with drag-reducing polymer. Exp. Therm. Fluid Sci. 79, 275–282. https://doi.org/10.1016/j.expthermflusci.2016.07.023.

Ahmed, S.A., John, B., 2021a. Dimensionless parameters to identify transition from stratified to non-stratified flow pattern in liquid–liquid horizontal pipe flow. Flow, Turbul. Combust. 107, 653–681. https://doi.org/10.1007/s10494-021-00245-2.

Ahmed, S.A., John, B., 2021b. Predictive correlations for heat transfer characteristics of oil-water horizontal pipe flow-an experimental study. J. Petrol. Sci. Eng. 204, 108733. https://doi.org/10.1016/j.petrol.2021.108733.

Al-Wahaibi, T., Angeli, P., 2007a. Transition between stratified and non-stratified horizontal oil-water flows. Part I: Stability analysis. Chem. Eng. Sci. 62, 2915–2928.

Al-Wahaibi, T., 2012. Pressure gradient correlation for oil-water separated flow in horizontal pipes. Exp. Therm. Fluid Sci. 42, 196–203. https://doi.org/10.1016/j.expthermflusci.2012.04.021.

Al-Wahaibi, T., Smith, M., Angeli, P., 2007b. Transition between stratified and nonstratified horizontal oil–water flows. Part II: mechanism of drop formation. Chem. Eng. Sci. 62, 2929–2940. https://doi.org/10.1016/j.ces.2007.01.036.

Al-Yaari, M., Soleimani, A., Abu-Sharkh, B., Al-Mubaiyedh, U., Al-Sarkhi, A., 2009. Effect of drag reducing polymers on oil–water flow in a horizontal Pipe. Int. J. Multiphas. Flow 35 (6), 516–524. https://doi.org/10.1016/j.ijmultiphaseflow.2009.02.017.

Angeli, P., Hewitt, G.F., 1998. Pressure gradient in horizontal liquid-liquid flow. Int. J. Multiphas. Flow 24, 1183–1203. https://doi.org/10.1016/S0301-9322(98)00006-8.

Biberg, D., Halvorsen, G., 2000. Wall and interfacial shear stress in pressure driven two-phase laminar stratified pipe flow. Int. J. Multiphas. Flow 26, 1645–1673. https://doi.org/10.1016/S0301-9322(99)00109-3.

Bochio, G., Cely, M.H., Teixeira, A.F.A., Rodriguez, O.M.H., 2021. Experimental and numerical study of stratified viscous oil–water flow. AIChE J. 67, 6. https://doi.org/10.1002/aic.17239.

Brauner, N., Moalem, D.M., Rovinsky, J., 1998. A two fluid model for stratified flows with curved interfaces. Int. J. Multiphas. Flow 24, 975–1004. https://doi.org/10.1016/S0301-9322(98)00005-6.

Brauner, N., 2001. The prediction of dispersed flows boundaries in liquid-liquid and gas-liquid systems. Int. J. Multiphas. Flow 27, 885–910. https://doi.org/10.1016/S0301-9322(00)00056-2.

Brinkman, H.C., 1952. The viscosity of concentrated suspensions and solutions. J. Chem. Phys. 20, 571. https://doi.org/10.1063/1.1700493.

Cai, X.M., Steyn, D.G., 1996. The von Kármán constant determined by large eddy simulation. Bound. Layer Meteor 78, 143–164. https://doi.org/10.1007/BF00122490.

Chakrabarti, D.P., Das, G., Ray, S., 2005. Pressure drop in liquid-liquid two phase horizontal flow: experiment and prediction. Chem. Eng. Technol.: Industrial Chem. Plant Equip. Proc. Eng. Biotechnol. 28 (9), 1003–1009. https://doi.org/10.1002/ceat.200500143.

Charles, M., Govier, G.W., Hodgson, G.W., 1961. The horizontal flow of equal density oil-water mixtures. Can. J. Chem. Eng. 39 (1), 27–36. https://doi.org/10.1002/cjce.5450390106.

Charles, M.E., Lilleleht, 1966. Correlation of pressure gradient for the stratified laminar-turbulent pipeline flow of two immiscible liquids. Can. J. Chem. Eng. 44 (1), 47–79. https://doi.org/10.1002/cjce.54504401100.

Clausse, A., de Bertodano, M.L., 2021. Natural modes of the two-fluid model of two-phase flow. Phys. Fluids 33, 033324. https://doi.org/10.1063/5.0046189.

Dasari, A., Anand, B.D., Ujjal, K.G., Ashok, K.D., Tapas, K.M., 2014. Correlations for prediction of pressure gradient of liquid-liquid flow through a circular horizontal pipe. J. Fluid Eng. 136, 1–12. https://doi.org/10.1115/1.4026582.

dos Santos, R.G., Mohamed, R.S., Bannwart, A.C., Loh, W., 2006. Contact angle measurements and wetting behavior of inner surfaces of pipelines exposed to heavy crude oil and water. J. Petrol. Sci. Eng. 51, 9–16. https://doi.org/10.1016/j.petrol.2005.11.005.

Dorao, C.A., Drewes, S., Fernandino, M., 2018. Can the heat transfer coefficients for single-phase flow and for convective flow boiling be equivalent? Appl. Phys. Lett. 112, 064101. https://doi.org/10.1063/1.50186599.

Dukler, A.E., Wicks, M., Cleveland, R.G., 1964. Frictional Pressure drop in two-phase flow. AIChE J. 10, 44–51. https://doi.org/10.1002/aic.690100118.

Edomwonyi-Otu, L.C., Angeli, P., 2014. Pressure drop and holdup predictions in horizontal oil–water flows for curved and wavy interfaces. Chem. Eng. Res. Des. 1–11. https://doi.org/10.1016/j.cherd.2014.06.009.

Elseth, G., 2001. An Experimental Study of Oil/water Flow in Horizontal Pipes. PhD Thesis. The Norwegian University of Science and Technology, Norway. http://hdl.handle.net/11250/231 212.

Grassi, B., Strazza, D., Poesio, P., 2008. Experimental validation of theoretical models in two-phase high-viscosity ratio liquid–liquid flows in horizontal and slightly inclined pipes. Int. J. Multiphas. Flow 34 (10), 950–965. https://doi.org/10.1016/j.ijmultip haseflow.2008.03.006.

Guzhov, A., Grishin, A.D., Medredev, V.F., Medredeva, O.P., 1973. Emulsion formation during the flow of two immiscible liquids. Neft.Chiz. 8, 58–61 (in Russian).

Hapanowicz, J., Polaczek, P., 2013. Convective heat transfer of a liquid dispersion system flowing in a pipe. Exp. Therm. Fluid Sci. 45, 1–7. https://doi.org/10.1016/j.expthermflusci.2012.11.007.

Hapanowicz, J., 2021. Two-phase liquid–liquid flow in the aspect of reduction of pumping power of hydrophobic substances with high viscosity. Energies 14, 2432. https://doi.org/10.3390/en14092432.

Hinze, J.O., 1975. Turbulence, 2d ed. McGraw-Hill, p. 790.

Ibarra, R., Markides, C.N., Matar, O.K., 2014. A Review of Liquid-Liquid Flow Patterns in Horizontal and Slightly Inclined Pipes, vol. 26, pp. 171–198. https://doi.org/10.1615/MultScienTechn.v26.i3.10.

Ibarra, R., Zadrazil, I., Matar, O.K., Markides, C.N., 2018. Dynamics of liquid–liquid flows in horizontal pipes using simultaneous two–line planar laser–induced fluorescence and particle velocimetry. Int. J. Multiphas. Flow 1–17. https://doi.org/10.1016/j.ijmultiphase flow.2017.12.018.

Knudsen, J.G., Katz, D.L.V., 1954. Fluid Dynamics and Heat Transfer. University of Michigan.

Liu, J.P., Zhang, H., Wang, S.H., Wang, J., 2008. Prediction of pressure gradient and holdup in small EÖtvÖs number liquid-liquid segregated flow. Chin. J. Chem. Eng. 16 (2), 184–191. https://doi.org/10.1016/S1004-9541(08)60060-9.

Lovick, J., Angeli, P., 2004. Experimental studies on the dual continuous flow pattern in oil-water flows. Int. J. Multiphas. Flow 30, 139–157. https://doi.org/10.1016/j.ijmultiphaseflow.2003.11.0 11.

Martinez, A.E., Arirachakaran, S., Shoham, O., Brill, J.P., 1988. Prediction of Dispersion Viscosity of Oil/Water Mixture Flow in Horizontal Pipes. In: 63rd Annual Technical Conference and Exhibition of the Society of Petroleum Engineers, TX, Oct. 2–5.

Mukhaimer, A., Al-Sarkhi, A., El-Nakla, M., Ahmed, W.H., A-Hadhrami, L., 2015. Pressure drop and flow pattern of oil-water flow for low viscosity oils: role of mixture viscosity. Int. J. Multiphas. Flow. https://doi.org/10.1016/

j.ijmultiphaseflow.2015.02 .018.
Nadler, M., Mewes, D., 1997. Flow induced emulsification in the flow of two immiscible liquids in horizontal pipes. Int. J. Multiphas. Flow 23, 55–68. https://doi.org/10.1016/S0301-9322(96)00055-9.
Ng, T.S., Lawrence, C.J., Hewitt, G.F., 2004. Friction factors in Stratified two-phase flows. Trans IChemE, Part A, Chemical Engineering Research and Design 82 (A3), 309–320. https://doi.org/10.1205/026387604322870426.
Oliemans, R., 2011. Oil-water liquid flow rate determined from measured pressure drop and water hold-up in horizontal pipes. J. Braz. Soc. Mech. Sci. Eng. 33, 259. https://doi.org/10.1590/S1678-58782011000500008.
Pal, R., 1993. Pipeline flow of unstabilized and surfactant-stabilized emulsions. AIChE J. 39 (11), 1754–1764. https://doi.org/10.1002/AIC.690391103.
Pal, R., Rhodes, E., 1989. Viscosity/concentration relationships for emulsions. J. Rheol. 33 (7), 1021–1045.
Richardson, S.M., 1989. Fluid Mechanics. Hemisphere Publishing Corporation, pp. 251–260.
Rodriguez, O.M.H., Baldani, L.S., 2012. Prediction of pressure gradient and holdup in wavy startified liquid-liquid inclined pipe flow. J. Pet. Sci. Eng. 96, 140–151. https://doi.org/10.1016/j.petrol.2012.09.007.
Rodriguez, O.M.H., Oliemans, R.V.A., 2006. Experimental study on oil-water flow in horizontal and slightly inclined pipes. Int. J. Multiphas. Flow 32, 323–343. https://doi.org/10.1016/j.ijmultiphaseflow.2005.11.001.
Rodriguez, I.H., Yamaguti, H.K.B., de Castro, M.S., Da Silva, M.J., Rodriguez, O.M.H., 2012. Drag reduction phenomenon in viscous oil-water dispersed pipe flow: experimental investigation and phenomenological modeling. AIChE 58. https://doi.org/10.1002/aic.12787.
Roscoe, R., 1952. The viscosity of suspensions of rigid spheres. Br. J. Appl. Phys. 3, 267. https://doi.org/10.1088/0508-3443/3/8/306.
Shi, J., Yeung, H., 2016. Characterization of liquid-liquid flows in horizontal pipes. AIChE J. https://doi.org/10.1002/aic.15452.
Sotgia, G., Tartarini, P., Stalio, E., 2008. Experimental analysis of flow regimes and pressure drop reduction in oil-water mixtures. Int. J. Multiphas. Flow 34 (12), 1161–1174. https://doi.org/10.1016/j.i.jmultiphaseflow.2008.06.001.
Strazza, D., Grassi, B., Demori, M., Poesio, P., 2011. Core-annular flow in horizontal and slightly inclined pipes: existence, pressure drops, and hold-up. Chem. Eng. Sci. 66 (12), 2853–2863. https://doi.org/10.1016/j.ces.2011.03.053.
Tan, J., Jing, J., Hu, H., You, X., 2018. Experimental study of the factors affecting the flow pattern transition in horizontal oil–water flow. Exp. Therm. Fluid Sci. 98, 534–545. https://doi.org/10.1016/j.expthermflusci.2018.06.020.
Telford, J.W., Businger, J.A., 1986. Comments on "Von Kármán's constant in atmospheric boundary layer flow: reevaluated.". J. Atmos. Sci. 43, 2127–2134.
Trallero, J.L.A., Sarica, C., Brill, J.P., 1997. A study of Oil/Water Flow patterns in horizontal pipes, SPE36609. In: Annual Technical Conference and Exhibition, CO, USA. https://doi.org/10.2118/36609-PA.
Ullmann, A., Brauner, N., 2006. Closure relations for two-fluid models for two-phase stratified smooth and stratified wavy flows. Int. J. Multiphas. Flow 32, 82–105. https://doi.org/10.1016/j.ijmultiphaseflow.2005.08.005.
Ullmann, A., Goldstein, A., Zamir, M., Brauner, N., 2004. Closure relations for the shear stresses in two-fluid models for laminar stratified flow. 30 (7–8),, 877–890. https://doi.org/10.1016/j.ijmultiphaseflow.2004.03.008.
Valle, A., Kvandal, H., 1995. Pressure Drop and Dispersion Characteristics of Separated Oil/water Flow. Proc. Of Int. Symp. on Two-phase Flow Modelling and Experimentation. Rome, Italy. ISBN:8877418524.
Vielma, M., Atmaca, S., Sarica, C., Zhang, 2008. Characterization of Oil-Water Flows in Horizontal Pipes, SPE109591, 2007 - SPE Annual Technical Conference and Exhibition. Anaheim, California, USA. https://doi.org/10.2523/109591-ms.
Wahid, M.F., Tafreshi, R., Khan, Z., Retnanto, A., 2021. Prediction of pressure gradient for oil-water flow: a comprehensive analysis on the performance of machine learning algorithms. J. Petrol. Sci. Eng. 208. https://doi.org/10.1016/j.petrol.2021.109265.
Wallis, G.B., 1969. One Dimensional Two-phase Flow. McGraw-Hill, N.Y., ISBN-13: 978-0070679429.
Ward, J.P., 1964. Turbulent Flow of Liquid - Liquid Dispersions: Drop Size, Friction Loss, and Velocity Distributions. Ph. D. thesis. Corvallis, Oregon State University, USA. http://hdl.handle.net/1957/11689.
Wright, C.H., 1957. Pressure Drop and Heat Transfer for Liquid - Liquid Dispersions in Turbulent Flow in a Circular Tube. MS Thesis. Oregon State College, Corvallis (USA).
Yang, Z., 2014. A Study of Viscous Oil and Water Flow. In: 9th North American Conference on Multiphase Technology, Banff, Canada.
Yang, J., Li, P., Zhang, X., Lu, X., Li, Q., Mi, L., 2021. Experimental investigation of oil–water flow in the horizontal and vertical sections of a continuous transportation pipe. Sci. Rep. 11, 20092. https://doi.org/10.1038/s41598-021-99660-8.
Yusuf, N., Al-Wahaibi, Y., Al-Wahaibi, T., Al-Ajmi, A., Olawale, A.S., Mohammed, I.A., 2012. Effect of oil viscosity on the flow structure and pressure gradient in horizontal oil–water flow. Chem. Eng. Res. Des. 90 (8), 1019–1030. https://doi.org/10.1016/j.cherd.2011.11.013.
Zigrang, D.J., Sylvester, N.D., 1985. A review of explicit friction factor equations. Transactions of the ASME. Journal of Energy Resources Technology. 107 (2), 280–283. https://doi.org/10.1115/1.3231190.
Zuber, N., Findlay, I., 1965. Average volumetric concentration in two-phase flow systems. Trans. J. Heat Transfer. ASME 87, 345–468. https://doi.org/10.1115/1.3689137.